Surface structure transitions on InAs and GaAs (001) surfaces

Hiroshi Yamaguchi and Yoshiji Horikoshi
NTT Basic Research Laboratories, Atsugi-shi, Kanagawa 243-01, Japan
(Received 29 November 1994)

Surface structure transitions on InAs and GaAs (001) surfaces are studied by using reflection high-energy electron diffraction (RHEED), scanning tunneling microscopy (STM), scanning electron microscopy (SEM), and Monte Carlo simulations. The RHEED study shows that the change in surface structure between As-stabilized (2×4) and In-stabilized (4×2) structures on InAs (001) is a discontinuous first-order phase transition with hysteresis, and that the discontinuous transition is not observed on GaAs surfaces. This phenomenon can be explained by a two-dimensional lattice-gas model assuming lateral interaction between surface species, and it is suggested that the lateral interaction is stronger with InAs than GaAs. The scanning tunneling microscopy observation indicates that this strong lateral interaction between surface species causes a thermally stable dimer-vacancy row structure on the InAs (2×4) surface. The reflection high-energy electron diffraction, STM, and SEM observation for misoriented InAs surfaces clarify the role of steps on the phase transition. The metastability of the InAs surface is shown to be reduced by monomolecular steps due to the finite size effects on the phase transition.

I. INTRODUCTION

(001)-oriented polar surfaces of compound semiconductors are important not only for the applications like the fabrication of quantum structures by molecular beam epitaxy (MBE), but also for semiconductor surface physics.[1,2] One of the most interesting surface physical properties is the variety of ways in which they undergo surface reconstruction. Analyses of GaAs surfaces have shown that these various surface structures are due to different surface stoichiometries.[3–7] Models of these structures have been proposed based on scanning tunneling microscopy (STM),[8,9] and reflection high-energy electron diffraction (RHEED) (Ref. 10) measurements, and also on theoretical calculations.[11–13]

The static properties of these surface structures have been studied in detail, but the dynamic properties of the phase transitions between different surface structures, have not received so much attention. Recent advances in MBE have made it possible not only to prepare clean surfaces but also to get important information about the dynamics of the phase transition by positively modulating the surface. For example, the surface can be modulated by depositing some species of atoms, slightly misorienting the surface axis, or introducing stress by forming heterointerfaces.

Phase transitions and the effects of surface modulation on them have been studied in depth for metals and elemental semiconductors like Ge or Si.[14–17] Order-disorder transitions and changes in surface structure by the deposition of different materials have been reported in detail. However, transitions on compound semiconductor surfaces are difficult to study because they can only be observed under molecular beam flux in an MBE chamber requiring the use of a complex experimental apparatus, and also because of the complexity of the transition itself.

In this paper, we discuss the phase transition between As-stabilized $(2 \times 4)/c(2 \times 8)$ and In-stabilized $(4 \times 2)/c(8 \times 2)$ structures [referred to as (2×4) and (4×2) for simplicity hereafter] on InAs (001) surfaces, which is more elemental than the corresponding phase transition on GaAs surfaces as shown in the following sections. This discussion is based on the results of experimental RHEED, STM, and scanning electron microscopy (SEM) measurements, and on theoretical Monte Carlo simulations with a two-dimensional lattice-gas model.

We focus on three aspects of the phase transition on InAs (001) surfaces. One is the mechanism that causes first-order discontinuous phase transitions on InAs (001) surfaces. In Secs. III and IV, the lateral interaction between surface species is shown to play an important role in the first-order phase transition. The second is the difference between InAs and GaAs. The discontinuous transition is observed only with InAs. We discuss the possible origins based on Monte Carlo simulations and atom-resolved STM observations in Secs. IV and V. The third is the role of steps on the phase transition. The influence of surface steps (the so-called finite size effect) and its anisotropic behavior is discussed in Secs. VI and VII.

II. EXPERIMENT

Observations were performed after growing more than 0.2 μm of an undoped or Si-doped buffer layer on undoped InAs, GaAs, and Si-doped GaAs substrates. The Si-doped samples were used mainly for STM observations. The doping level was kept below 5×10^{17} cm^{-3} in order to avoid the influence on surface structure uniformity.[18] Conventional surface treatment was performed before MBE growth.

Reflection high-energy electron diffraction observa-

tions were made in the MBE chamber just after the growth of the buffer layer. The RHEED specular beam intensity was measured and RHEED pattern was monitored as a function of substrate temperature with As_4 beam and no In/Ga beam supplied on the surface. To detect the diffracted and reflected electron beam intensity, we used a Faraday cup-shaped electrode and a phosphor screen. The former has a wide dynamic range and the latter allows the two-dimensional diffraction pattern to be observed.[19] The pattern on the phosphor screen was analyzed by an image processor to measure the intensity variation in the diffraction patterns.

Because the RHEED intensity can largely depend on the diffraction conditions owing to multiple scattering effects, we compared the results obtained under different diffraction conditions. We confirmed that the results do not depend on the conditions. The typical conditions were an electron acceleration voltage of 10 kV to 20 kV, an incident azimuth of [110] or [1$\bar{1}$0] $\pm 10°$, and an incident angle of 1.0° to 2.0°.

For the STM and SEM observation, the buffer layer was grown in a separate MBE chamber. The sample was passivated by an As-protective layer by cooling it to $-10\,°C$ in an As flux after MBE growth.[20] The sample was then transferred through air to the STM or SEM system, and observation was performed after removing the As layer by thermal annealing. The STM system was directly connected to another MBE chamber through an ultrahigh vacuum. Thin layers were grown on the samples in this MBE chamber to prepare as-grown surfaces.

We used a JEOL JSTM-4500VT STM system, which can operate in ultrahigh vacuum conditions at temperatures up to 900 °C.[21] The base pressure was 2×10^{-10} Torr during observation. An electrochemically etched tungsten tip without special treatment was used as a probe. Before the observation of InAs or GaAs surfaces, the tip was annealed by heating a Si wafer (~800 °C), which was placed about 0.5 mm away from the tip.

An ultrahigh vacuum SEM instrument equipped with a field emission electron gun (a modified Hitachi S-800) was used for surface imaging.[22–24] The base pressure during SEM observation was 8×10^{-10} Torr without heating the As cell. A secondary electron (SE) detector biased at 10 kV was placed to one side of the specimen. The working distance between the objective lens and the specimen was about 10 mm. A 25-kV electron beam with a current of 0.1 nA was used, and the best resolution was about 5 nm. The sample was mounted on a Si substrate, which acted as a resistive heater, after exposing the passivated sample to air from the MBE chamber. The SEM observation was performed while increasing and decreasing the sample temperature with an As_4 beam of about 1×10^{-6} Torr supplied on the sample by an effusion cell installed in the SEM chamber.

In all the measurements, the substrate temperature was measured by infrared pyrometers with wavelengths of 0.8 μm for GaAs substrates and 2.0 μm for InAs substrates. During STM observations of heated GaAs samples, the 2.0-μm pyrometer was used. The temperature was calibrated with the 0.8-μm pyrometer in the high temperature range of 400 °C–600 °C.

III. RHEED MEASUREMENT OF FIRST-ORDER PHASE TRANSITION

A. Discontinuous transition on the InAs surface

The RHEED specular beam intensity of InAs and GaAs (001) surfaces was measured under an As_4 pressure of about 2.5×10^{-6} Torr (Fig. 1). We first increased the sample temperature and then decreased it. Since the rate of temperature change was about 1 °C/min, thermal equilibrium was established at each observation. In fact, the hysteresis width was independent of the speed of temperature change in the range from 0.5 to 2 °C/min. This means the surface was in thermal equilibrium throughout the transition. For both InAs and GaAs, we observed a (2×4) pattern at low substrate temperature, which corresponds to an As-stable surface, and a (4×2) pattern, which corresponds to an In/Ga-stable surface, at high substrate temperatures. There is a large difference in the transition region.[25]

With InAs, the electron reflectivity changed discontinuously as a function of temperature, with a 10 °C-wide hysteresis. This result was obtained reproducibly, since the reflectivity changes in two different runs coincide perfectly (see Fig. 1). This result suggests that

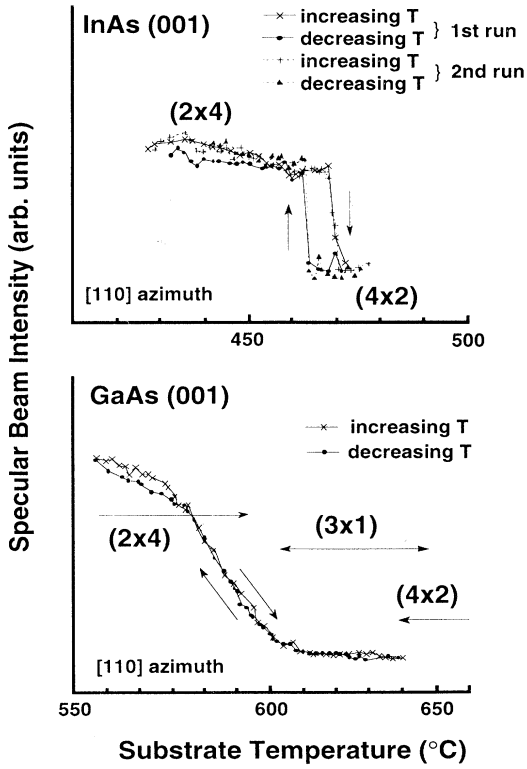

FIG. 1. Reflection high-energy electron diffraction specular beam intensity vs substrate temperature of exactly oriented InAs and GaAs (001) surfaces with a fixed As pressure of about 2.5×10^{-6} Torr.

the surface structure transition between As-stable (2×4) and In-stable (4×2) is a first-order phase transition. In fact, a (2×4)/(4×2) mixed structure was observed during the discontinuous transitions both from (2×4) to (4×2), and vice versa, which also indicates that the transition is first order. Moison *et al.*[26] reported that the reconstruction transition for InAs (001) has a hysteresis cycle. Our results clearly show that a physical parameter, i.e., the electron reflectivity, has a discontinuous dependence on substrate temperature.

Surface reconstruction is a function of surface coverage, and surface coverage is a function of substrate temperature. The first-order transition for InAs raises two possibilities: (1) the surface reconstruction (or surface structure in general) is a discontinuous function of surface coverage, (2) the surface coverage is a discontinuous function of substrate temperature. As deduced from STM observations in Sec. VI B, the height profile across the boundary between (2×4) and (4×2) domains suggests that the As actually desorbs from (2×4) domains to form (4×2) structures. Therefore, the surface coverage itself is a discontinuous function of sample temperature.

With GaAs, the specular beam intensity changed gradually as a function of the temperature, passing through an intermediate (3×1) structure of which the fractional order line was not as intense as that of (2×4) or (4×2). This shows that the (3×1) is a disordered structure. The transition is continuous for GaAs (001) and the disordered (3×1) structure can exist for any degree of As coverage between As-stable (2×4) and Ga-stable (4×2) surfaces. In the case of a GaAs surface, prolonged annealing of the sample with a (4×2) surface deteriorated the surface quality; the RHEED pattern becomes spotty probably due to the formation of Ga droplets.[27] [This deterioration was not observed with InAs surfaces even when we annealed them at 30 °C higher than the transition temperature from (2×4) to (4×2).] We started to decrease the GaAs sample temperature as soon as (3×1)/(4×2) mixed structures became visible. Even with such careful treatment, a small amount of hysteresis narrower than 5 °C was also observed for GaAs only in the measurement just after growth of the buffer layer. Small hysteresis was also reported by Leprince *et al.*[28] for the fractional order beam intensity of (2×4) RHEED patterns. At least in our measurements of specular beam intensity, no hysteresis was observed from the second run as shown in Fig. 1 [This hysteresis may be caused by a surface step structure change from (2×4) to (4×2), which was actually observed in the SEM analysis of InAs as mentioned in Sec. VII E.]

For GaAs, the boundaries between (2×4) and (3×1) structures did not show any mixed structures between them. This also indicates that the transition between (2×4) and (3×1) is not first order. At the boundary between (3×1) and (4×2), on the other hand, a mixed RHEED pattern was observed. Therefore, the transition can be a first-order one between (3×1) and (4×2). However, the transition was not discontinuous; i.e., the mixed surface can be maintained by keeping the temperature constant. (In the case of InAs, we could not maintain the mixed structure, because the transition proceeds quickly even at a constant temperature.) Even a first-order transition can be continuous, due to the finite size effect caused by the surface atomic steps, as reported for the order-disorder transition on an Si (111) surface.[29,30] The transition between (3×1) and (4×2) on a GaAs surface becomes continuous, probably due to finite size effects. (We will discuss this point in Sec. VII.) Therefore, the stoichiometry change is supposed to be continuous throughout (2×4), (3×1), and (4×2) on GaAs surfaces.

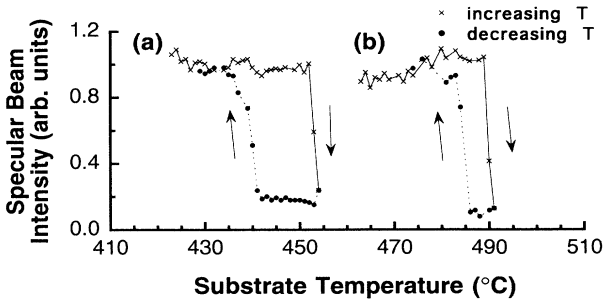

FIG. 2. Reflection high-energy electron diffraction specular beam intensity as a function of substrate temperature for an exactly oriented InAs (001) surface with As pressures of (a) 1.0×10^{-6} and (b) 7.8×10^{-6} Torr.

B. As pressure dependence

Figure 2 shows the temperature dependence of specular beam intensity for an InAs (001) surface at two different As pressures. The temperature at which the surface structure changes is determined by the equilibrium between the desorption of As from the surface and the adsorption of As supplied from the effusion cell. Therefore, this temperature (referred to as the transition temper-

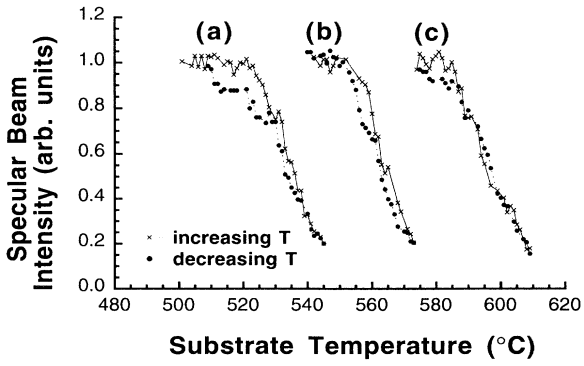

FIG. 3. Reflection high-energy electron diffraction specular beam intensity as a function of substrate temperature for an exactly oriented GaAs (001) surface with As pressures of (a) 9.0×10^{-8}, (b) 3.9×10^{-7}, (c) 2.8×10^{-6} Torr.

ature hereafter) increases with As pressure, as actually observed in the experimental results. In addition, the hysteresis width decreased as the As pressure increased. This phenomenon shows that the metastable region accompanying the first-order phase transition was smaller at higher substrate temperature due to the entropy effect as discussed in Sec. IV B.[31]

On the other hand, no significant change was observed with GaAs, except for the increase of transition temperature with As pressure (Fig. 3). Little hysteresis was observed because these were the first measurements made after the growth of a buffer layer, as mentioned in Sec. III A. The width increases as the As pressure decreases, suggesting that the hysteresis is caused by kinetics.

IV. LATTICE-GAS MODEL AND MONTE CARLO SIMULATION

The lateral interaction between neighboring atoms plays an important role in the phase transitions. We tried to explain the first-order phase transition on InAs surfaces by a two-dimensional lattice-gas model that takes lateral interaction between surface species into account. The Bragg-Williams approximation[32] was first used to roughly understand the phenomenon, and a detailed Monte Carlo simulation was also used to fit the obtained As pressure dependence of transition temperatures for InAs surfaces.

A. Lattice-gas model and Bragg-Williams approximation

The actual surface processes for the desorption and adsorption of As atom/molecules are very complicated, the latter involving numerous subprocesses such as the decomposition of As_4 molecules to As_2 molecules, their surface migration, the decomposition of As_2 molecules into As atoms, and their reaction with In atoms. Surface reconstruction makes these processes even more complicated. To simplify the situation, we made the following assumptions.

(a) *The desorption and adsorption of As atoms occurs within units which form a rectangular lattice on the surface.* Scanning tunneling microscopy observations show that As-covered (2×4) surfaces contain As dimers and dimer vacancies.[8,9,33,34] The As units can, therefore, be individual As atoms or groups of one or more As dimers.

(b) *In the temperature range used for these experiments, the sticking coefficient of As units on an As-stable surface is negligibly small.* We assume that the adsorption of an As unit can occur only on an In-exposed site. In other words, no As unit can adsorb at an As-covered site.

(c) *A surface As unit interacts with In atoms in the lower atomic layer and with neighboring As units.*[35] In the following, the former is referred to as vertical interaction and the latter as lateral interaction. We specify the two-dimensional surface site position by (n,m) (the position along the [110] and [1$\bar{1}$0] directions, respectively), and the existence of an As unit at this position is expressed by $\eta_{n,m}$, which takes the value of 1 for existence and 0 for absence. The Hamiltonian of the system is then given by

$$H = -\sum_{n,m} E_s \eta_{n,m} - \sum_{n,m} E_i(\eta_{n,m}\eta_{n+1,m} + \eta_{n,m}\eta_{n,m+1}). \tag{1}$$

Here, E_s is the energy of vertical interaction, and E_i gives the energy of lateral interaction (Fig. 4). This Hamiltonian is identical to that of the two-dimensional Ising model, as is easily shown by rewriting the formula using the commonly used Ising spin, $\sigma_{n,m} = 2\eta_{n,m} - 1$. It is well known that the two-dimensional Ising model represents second-order phase transitions. This is because the considered transition is an order-disorder one which is not identical with our case. In our case, the upper and lower spins in the Ising model correspond to As-occupied and to As-empty sites. The transition can be first-order because the equilibrium of this two-dimensional gas phase with a vapor phase (i.e., As flux) was considered by allowing the particles to move from one phase to the other.

Analytical treatment of phase transition is generally very difficult, and exact solutions can only be obtained for a small number of systems like an Ising model with no magnetic fields.[36] Hence, a suitable approximation must be used in many cases. Here, the Bragg-Williams approximation, which is one of the most widely used methods for phase transition systems, was applied to qualitatively analyze the phenomenon.

The Hamiltonian (1) gives the following distribution function:

$$Z(T,N) = \sum_{[\eta]} \exp\left\{ \left[\sum_{n,m} E_s \eta_{n,m} + \sum_{n,m} E_i(\eta_{n,m}\eta_{n+1,m} + \eta_{n,m}\eta_{n,m+1}) \right] \Big/ kT \right\}. \tag{2}$$

Here, the summation on η is carried for every set of $\eta_{n,m}$, which gives the same total number of adsorbed As units, N, i.e.,

$$N = \sum_{n,m} \eta_{n,m}. \tag{3}$$

It is impossible to perform this summation exactly. The

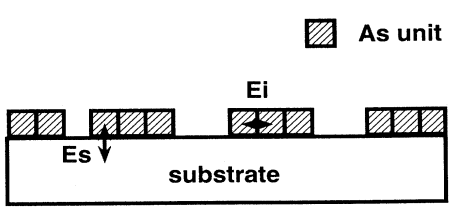

FIG. 4. Schematic illustration of the two-dimensional lattice-gas model used in this approximation.

total lateral interaction energy is approximated as being proportional to the square of the total number of adsorbed As units, N^2, in the Bragg-Williams approximation. The reason is that the number of neighboring As unit pairs is proportional to N^2 if we assume the adsorbed As units distribute randomly on the surface. Therefore, this approximation is effective only at small values of lateral interaction energy, E_i. By using the As-unit coverage, $\theta = N/N_0$ (N_0 is a total number of As unit sites), the total energy can be expressed by

$$E = -N_0(E_s\theta + 2E_i\theta^2). \tag{4}$$

The coefficient 2 of the second term in the parentheses was determined in order for the total energy to be $-N_0(E_s + 2E_i)$, with the value of θ of 1 as derived from Eq. (1). The distribution function, $Z(T, N)$, can be easily derived from this formula:

$$Z(T,N) = \sum_{N=\text{fixed}} \exp[N_0(E_s\theta + 2E_i\theta^2)/kT] = \frac{N_0!}{N!(N_0 - N)!} \exp[N_0(E_s\theta + 2E_i\theta^2)/kT]. \tag{5}$$

We have to consider the equilibrium of these adsorbed As-units phase with the As_4 flux supplied to the surface. The As_4 molecules supplied from the effusion cell are not thermodynamically in equilibrium with the surface. This is not only because the supplied As_4 is not an As unit, but also because the energy distribution of supplied As_4 is not determined by substrate temperature but by cell temperature, and the desorbed As is not readsorbed on the surface. To treat the equilibrium in a thermodynamic framework, we consider an As-unit monatomic gas with a constant pressure, p, and with the same temperature as the substrate. From Eq. (5), the chemical potential of adsorbed As units is given by

$$\mu = -kT\frac{\partial}{\partial N}\ln Z(T,N) = kT\ln\frac{\theta}{1-\theta} - E_s - 4E_i\theta. \tag{6}$$

On the other hand, the chemical potential of the monatomic gas phase is

$$\mu_g = -kT\ln\left[\left(\frac{2\pi mkT}{h^2}\right)^{3/2}\frac{kT}{p}\right] \equiv -kT\ln[C(T)/p]. \tag{7}$$

Therefore, the equilibrium condition is

$$p = C(T)\frac{\theta}{1-\theta}\exp\{-[E_s + 4E_i\theta]/kT\}. \tag{8}$$

This isotherm is known as the Fowler-Guggenheim isotherm.[32] The temperature dependence of the right hand side of this equation is due mainly to the exponential part. The dependence from $C(T)$ is very small, at least in the temperature range discussed here. We simply consider it as a constant, C, for simplicity hereafter.

Figure 5 shows the calculated variation of $\ln[p/C] + E_s/kT$ as a function of the As-unit coverage θ. We changed the values for $\alpha = E_i/kT$. The results show

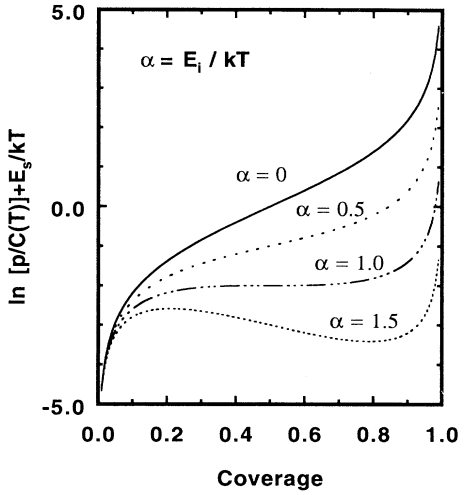

FIG. 5. Calculated $\ln[P/C] + E_s/kT$ as a function of As unit coverage for some values of $\alpha = E_i/kT$.

that a region with negative slope exists for values of α larger than 1. This means that there are two equilibrium As-unit coverages θ at a given As pressure p and temperature T for strong lateral interaction. This is the origin of the hysteresis observed in the first-order phase transition on InAs surfaces. The strong lateral interaction between surface As species makes the adsorbed phase metastable.

The first-order transition occurs if the value of α at the transition temperature ($\equiv T_t$) is larger than 1. From the condition that the coverage θ is 0.5 at the transition temperature T_t in Eq. (8), the temperature is determined by the equation,

$$p = C\exp[-(E_s + 2E_i)/kT_t]. \tag{9}$$

Hence, the transition temperature is a function of $E_s + 2E_i$, which we call the average interaction energy hereafter. The condition of the first-order transition is then

$$\frac{E_i}{E_s + 2E_i}\ln\frac{C}{p} > 1. \tag{10}$$

Therefore, *the transition becomes first-order if the ratio of lateral interaction energy to average interaction energy (or transition temperature) is sufficiently large.* The exact value of the right hand side is 1.76, which was obtained by Onsager with no approximation.[36]

As shown here, the lattice-gas model can reproduce the first-order phase transition if the lateral interaction energy is large enough. Next, the question arises: what is the origin of the difference between InAs and GaAs? If we rewrite the critical condition of Eq. (10) in terms of transition temperature T_t instead of average interaction energy, we obtain

$$\frac{E_i}{kT_t} > 1 \text{ (or 1.76 for Onsager solution).} \tag{11}$$

Hence, even if the lateral interaction, E_i has similar values both for InAs and GaAs, the transition can be first-order for InAs and continuous for GaAs because the transition temperature, T_t is lower for InAs than GaAs. In the next subsection, we discuss this point again, based on the detailed values for interaction energies.

B. Monte Carlo simulation

For quantitative analysis, we performed Monte Carlo simulation with the lattice-gas model used in the previous section.[37] To carry out the simulation, we also had to assume values for the kinetics of the reaction, i.e., the desorption and adsorption rates. From Eq. (1) and the principle of detailed valance, the following equation should be satisfied:

$$\frac{R_{d:n,m}}{R_{\mathrm{ad}:n,m}} = C_{st} \exp[-(E_s + N_{n,m}E_i)/kT]. \quad (12)$$

Here, $R_{d:n,m}$ is the desorption rate of the As unit occupying the site position (n,m), $R_{\mathrm{ad}:n,m}$ is the adsorption rate of the As unit to the empty site (n,m), where $N_{n,m}$ $(= \eta_{n+1,m} + \eta_{n-1,m} + \eta_{n,m+1} + \eta_{n,m-1})$ is the number of neighboring sites occupied by As units, and C_{st} is a constant. The simplest assumption is the following.

(d) *The adsorption rate, R_{ad}, is independent of temperature, T, and the number of neighboring occupied sites, $N_{n,m}$, and proportional to the As_4 pressure, P_{As}, i.e.,* $R_{\mathrm{ad}} = aP_{\mathrm{As}}$. This corresponds to a zero activation barrier between gas phase and adsorbed phase (Fig. 6). Therefore, the adsorption and desorption rates are given by

$$R_{\mathrm{ad}} = aP_{\mathrm{As}}, \quad (13)$$

$$R_{d:n,m} = \nu \exp[-(E_s + N_{n,m}E_i)/kT]. \quad (14)$$

This assumption of an Arrhenius-type reaction rate dependence is basically identical with the solid-on-solid model used in the growth simulation,[38,39] although the hopping process of adsorbates was not taken into account.

We basically used the Monte Carlo simulation algorithm proposed by Maksym to reduce the computation time.[40] Figure 7 shows the calculated As-unit coverage as a function of substrate temperature with $R_{\mathrm{ad}} = 2$ s^{-1}, $\nu = 10^{17}$ s^{-1}, and $E_s + 2E_i = 2.5$ eV. The temperature was first increased and then decreased at a rate of 1 °C/sec. The lattice size was 72×72 and the periodic boundary condition was used. If the size is too small, the finite size effect on the phase transition becomes significant. We confirmed that the results obtained with 50×50 and 100×100 lattices were identical. Therefore, the size is large enough to avoid this effect. We studied the dependence of lateral interaction energy, E_i. The results show that the transition is discontinuous with hysteresis for values of E_i larger than 0.12 eV, and is continuous when E_i is smaller than the critical value. This is identical with the results obtained in the previous subsection, and shows that strong lateral interaction causes a discontinuous first-order transition. The critical condition, which corresponds to equation (10), is now

$$\frac{E_i}{E_s + 2E_i} \ln \frac{\nu}{R_{\mathrm{ad}}} > 1.76. \quad (15)$$

From this equation, the transition is first-order when E_i is larger than 0.115 eV, which is close to the value of 0.12 eV obtained from the simulation. In the special case E_i =0, the Langmuir isotherm was obtained,

$$R_{\mathrm{ad}} = \frac{\theta}{1-\theta}\nu \exp(-E_s/kT). \quad (16)$$

The calculated results coincide perfectly with this curve. These two coincidences indicate the reliability of our cal-

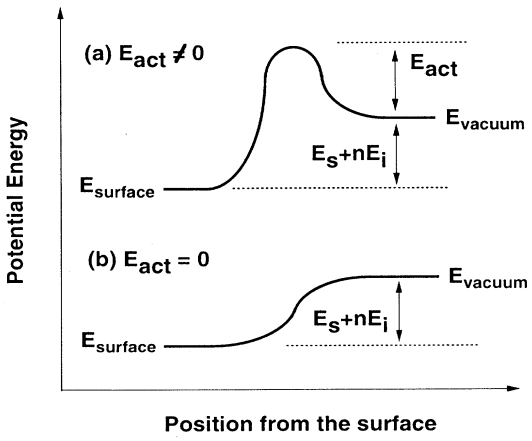

FIG. 6. Schematic illustration of the potential energy diagram between vacuum and surface: (a) is the general case with an activation barrier of E_{act} between them, and (b) corresponds to the assumption with no activation barrier is used in our calculations.

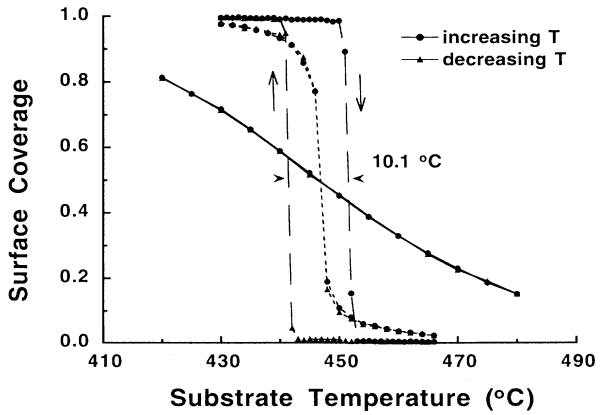

FIG. 7. Calculated coverage of As units on an exactly oriented surface as a function of substrate temperature when E_i is 0 (solid curve), 0.1 (dotted curve), and 0.16 eV (dashed curve).

culation.

To check the validity of the model, we compared the experimental and theoretical dependence of transition temperature on As pressure. Four parameters, E_s, E_i, a, ν were fitted to reproduce the experimental As pressure dependence. Among these parameters, a and ν are not independent. If we change these values without changing the ratio a/ν, the calculated transition temperature does not change because this change simply corresponds to the scaling of time. Therefore, the independent parameters are E_s, E_i, and a/ν.

Figure 8 shows the experimental and simulation results of the dependence of transition temperature on As pressure. The results coincide perfectly with the values for interaction energies of $E_s = 2.16$ eV and $E_i = 0.14$ eV. This coincidence is not obvious, because there are only three independent fitting parameters, E_s, E_i, and a/ν as mentioned above, in contrast to the four degrees of freedom of the two lines (which are actually curved lines, but can be approximated by straight lines in this temperature range). Therefore, this coincidence shows the validity of our model.

Figure 8 shows the phase diagram for surface structures on an InAs (001) surface. The upper-right region corresponds to an As-covered (2×4) surface, and the bottom-left region corresponds to an In-covered (4×2) surface. The region between lines L_1 and L_2 in the figure corresponds to the bistable region in which both As-covered (2×4) and In-covered (4×2) surfaces exist metastably. Onsager's critical condition, Eq. (11), shows that the discontinuous-continuous transition occurs at the critical temperature, $T_c = 0.567E_i/k$. This predicts that the transition between these two surfaces is not a first-order discontinuous transition at temperatures higher than T_c. Simple calculation shows that T_c is about 600 °C in this case, and an As pressure of 5.0×10^{-4} Torr is necessary to see this change in the order of the transition. In the present experiments, it was difficult to get such a high As pressure with our MBE system.

The next question is can the difference between InAs and GaAs be explained only from the difference in T_t? This point was already mentioned in Sec. IV A. From Eq. (11), the origin of the difference between InAs and GaAs can be both E_i and T_t. T_t is higher for GaAs than for InAs at the same As pressure, reflecting the difference in bond strength between In–As and Ga–As. If the lateral interaction E_i has the same value of 0.14 eV both for GaAs and InAs, the order-disorder transition occurs at about 600 °C independent of the vertical interaction, E_s, and frequency factor, ν. However, the specular beam intensity curve for GaAs (Fig. 3) suggests that the transition cannot be discontinuous even if the temperature is lower than this critical temperature. Therefore, the origin of the difference between GaAs and InAs seems not only to be T_t but also E_i itself. In other words, the lateral interaction, E_i, seems to be stronger for InAs than GaAs. In the next section, the origin of this difference in the lateral interaction energy, E_i, is discussed based on atomic-resolution images obtained by room-temperature STM observations.

V. MICROSCOPIC ORIGIN OF FIRST-ORDER TRANSITION

We studied the surface microscopic structures of InAs and GaAs by using STM to find the influence of the difference in lateral interaction on the atomic structure, enabling us to gain an understanding of the origin of the different lateral interaction between InAs and GaAs at the microscopic level.

A. Atomic-resolution STM imaging

Figure 9 shows a typical STM image of the InAs surface after growth. The sample was prepared by growing a thin (~10 nm) buffer layer after removing the As pro-

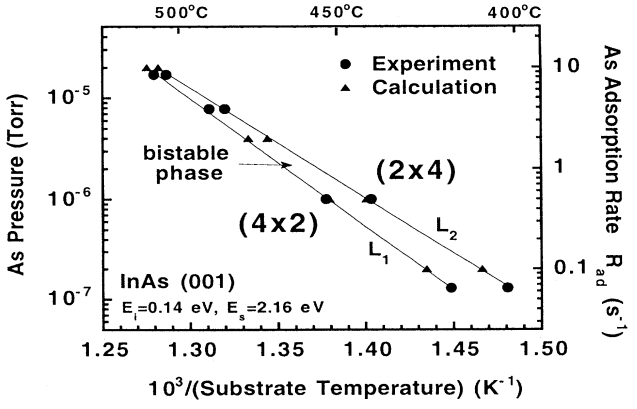

FIG. 8. Phase diagram of an InAs (001) surface obtained by RHEED observation (circles) and Monte Carlo simulation (triangles). L_1 and L_2 are guidelines representing the phase boundaries from (2×4) to (4×2) and from (4×2) to (2×4), respectively.

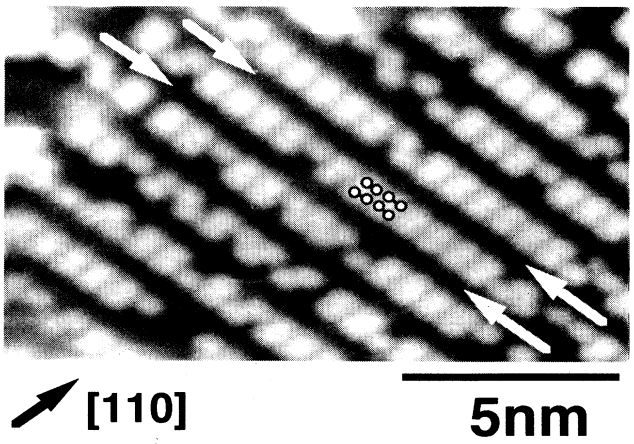

FIG. 9. Scanning tunneling microscopy image of an InAs (2×4) surface just after growth. The sample bias was −3.0 V and the tunneling current was 0.08 nA.

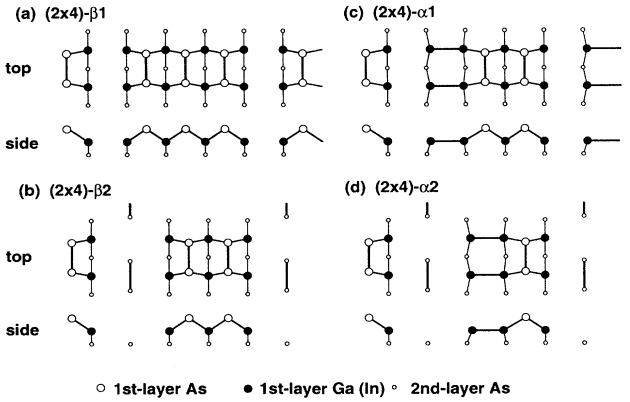

FIG. 10. Schematic representations of As-rich (2×4) structures with As coverages of 0.75 (a and b) and 0.5 (c and d). The top views and side views are both represented.

tective layer in the MBE chamber connected directly to the STM chamber by an ultrahigh vacuum. The image shows that the surface mainly consists of two As dimers. This structure is basically identical with that observed for GaAs surfaces.[18,33,34]

There are many uncertainties about the atomic arrangements of (2×4) structures. Arrangements with dimer-vacancy row structures for (2×4) reconstruction have been proposed by Chadi[11] and Farrell and Palmstrøm.[10] Theoretical consideration shows that these structures are energetically favorable.[11–13,41] In Chadi's model, three As dimers and one-dimer vacancy [Fig. 10(a)], or two As dimers and two-dimer vacancies [Fig. 10(b)] make up one (2×4) unit cell. Hereafter, we refer to these structures as (2×4)-β1 and (2×4)-β2, respectively. The effective As coverages for these two structures are both 0.75, because, even in the latter case, two As atoms in the layer one monolayer below form one dimer in the vacancy row as shown in Fig. 10(b). First principle calculations for these two structures recently verified that the three-dimer based structure, (2×4)-β1, has higher total energy than two As-dimer based (2×4)-β2 structures because of the electrostatic interaction between empty Ga dangling bonds and As lone pairs.[41] This

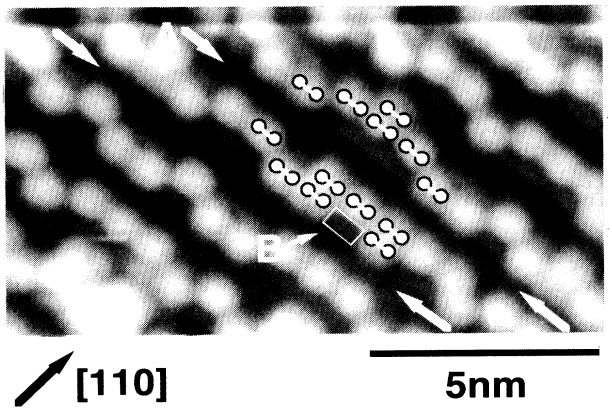

FIG. 11. The STM image of an InAs (001) (2×4) surface annealed at 340 °C. The sample bias voltage was −2.0 V and the tip current was 0.10 nA. The arrows labeled "A" show the dimer-vacancy rows, and As dimers are depicted on the image following the expected model. The arrow labeled "B" indicates the exposed In layer, one atomic layer below the top As layer.

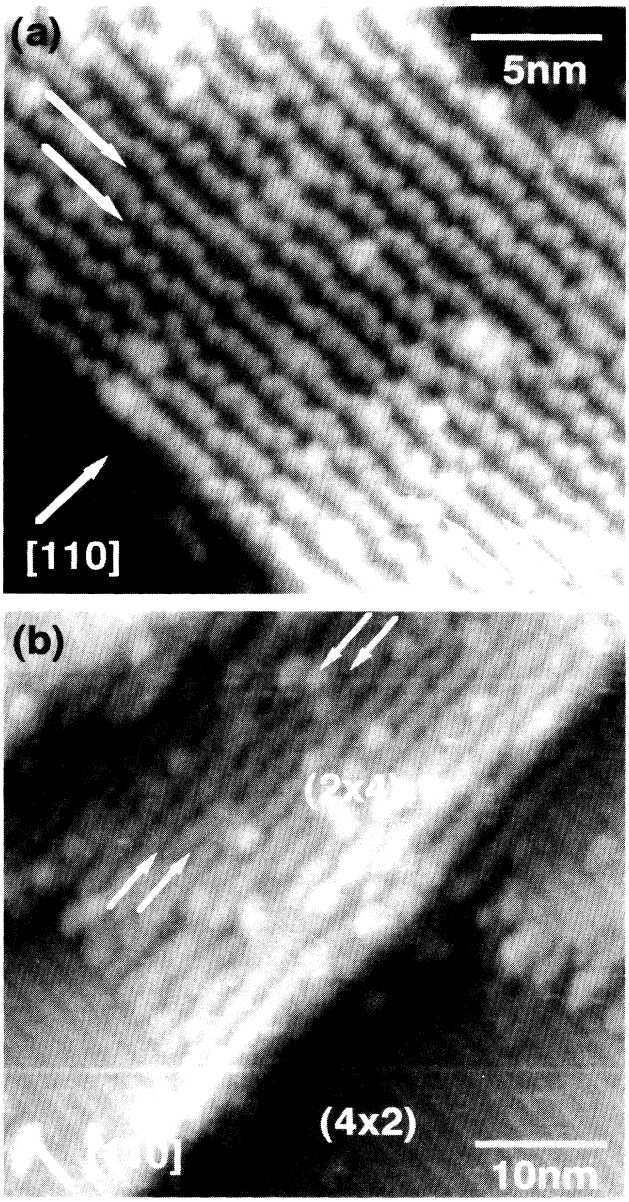

FIG. 12. The STM images of InAs (001) surfaces annealed at (a) 340 °C and (b) 370 °C. These images were obtained with bias voltages of −2.4 V and −3.0 V and with tip current of 0.10 nA and 0.08 nA, respectively. The arrows indicate As dimer-vacancy rows.

is consistent with the STM observation that only two As-dimer-based structure can be observed for various preparation conditions. With Farrell's two-dimer model, on the other hand, the As coverage is 0.5 because the Ga (In) atoms in the lower atomic layer are exposed and form Ga (In) dimers in the dimer-vacancy rows [(2×4)-α1 in Fig. 10(c)].

The InAs (2×4) structure just after the growth consists mainly of two As dimers, corresponding to (2×4)-β2 or (2×4)-α1. However, the STM image of the InAs (2×4) surface after heating to 340 °C for 10 min shows different atomic structures (Fig. 11).[42] This overheating caused As to desorb from the surface. It is clear from Fig. 11 that *the As-dimer rows consist mainly of single As dimers in the annealed sample,* showing that the single As-dimer structure was formed by heat-induced As desorption.

An In atomic layer was observed in the vacant site of an As dimer (B in Fig. 11), but the As-dimer-vacancy row (A's in Fig. 11) is lower than this In layer, indicating that this one-dimer structure was formed by the desorption of As atoms from the top layer of Chadi's (2×4)-β2 structure. This result suggests that the (2×4) structures of InAs (001) with higher As coverage, which should be obtained just after growth (Fig. 9), are (2×4)-β2, and also that annealing does not result in the (2×4)-α1 structure but instead causes single As-dimer structures [(2×4)-α2 in Fig. 10(d)], which also have an effective As coverage of 0.5.

B. Annealing effects

It should be noted that the dimer-vacancy row is very straight over a wide range on the surface especially for annealed samples, although the single As-dimer row is not straight. Figure 12(a) shows a wider area of the same surface shown in Fig. 11. The dimer-vacancy rows are perfectly straight for more than 50 nm. In other words, there are dimer-vacancy rows without kinks over a wide range. Further annealing results in In-covered (4×2) domains in (2×4) structures [Fig. 12(b)]. Even with such low As coverage, the dimer-vacancy rows are very straight. It is reasonable to conclude from these results that kinks do not form easily in the dimer-vacancy rows on InAs (2×4) surfaces.

On GaAs (2×4) surfaces, on the other hand, the kinks are easily formed by thermal annealing. Figure 13 shows STM images of a GaAs (2×4) surface, after the growth in the MBE chamber, which is directly connected with the STM chamber (a), and after annealing at 490 °C for 1 min (b). The kink density increased during annealing. This tendency was also reported by Zhou *et al.*[34]

These results show that the formation of single-dimer structures [(2×4)-α2] is significant for InAs and that kinks in the dimer-vacancy rows are significant for GaAs when the samples are annealed. This difference in the formation of defects in the surface periodic structures indicates the different lateral interactions between InAs and GaAs. High coherence in the fourfold periodicity of the InAs (2×4) structure shows that the lateral interaction is stronger in this surface than in GaAs. It was reported by Hashizume *et al.*[43] that a GaAs (2×4) surface prepared at higher substrate temperature has a (2×4)-α1 structure, not a (2×4)-α2 structure. This means that annealing changes the surface structure from (2×4)-β2 to (2×4)-α1, and that the disorder was induced by this structure transition. This seems reasonable because the formation energy of kinks in the dimer-vacancy rows is expected to be higher for (2×4)-β2 than for (2×4)-α1, which has a shallower vacancy row. The same difference is also expected between (2×4)-α2 and (2×4)-α1, i.e., the formation energy is expected to be higher for (2×4)-α2 than for (2×4)-α1. This explains why the dis-

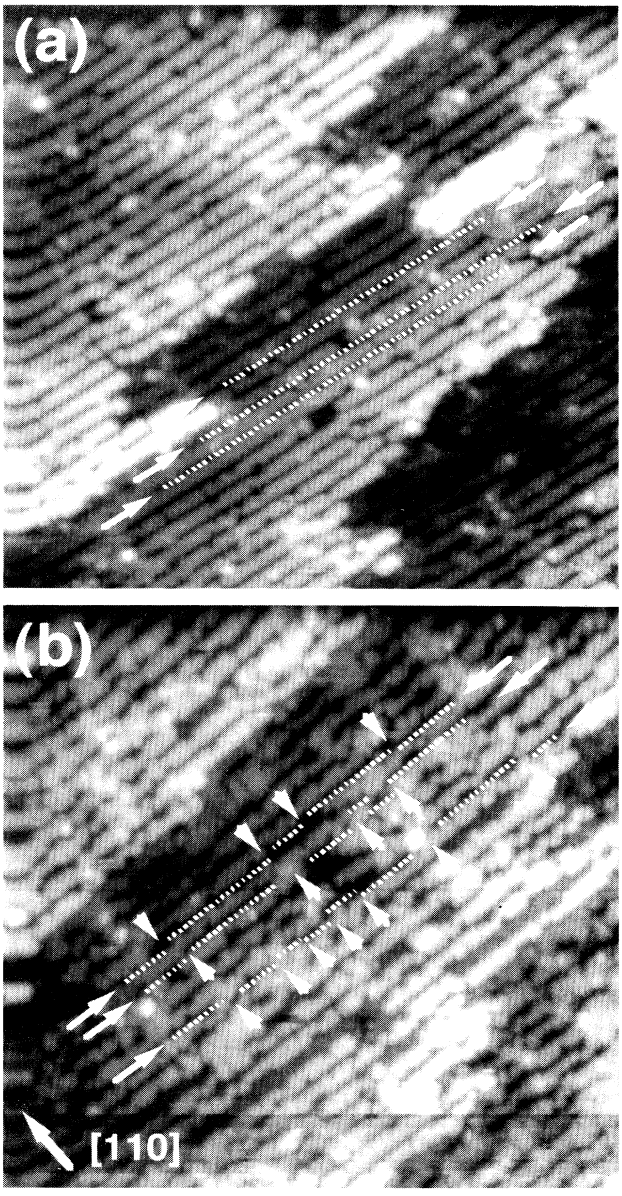

FIG. 13. The STM images of GaAs (001) surfaces (a) just after the growth and (b) after annealing at 490 °C for 1 min. The arrows indicate As dimer-vacancy rows, which are straight in (a) but include some kinks in (b).

order is not induced on InAs (001) surface. Although it is unclear why the preferred (2×4)-α structures of InAs and GaAs are different, the origin of the highly coherent (2×4) structure of InAs, and therefore the strong lateral interaction between surface species, can be this difference in the atomic structure of the (2×4)-α surface.

VI. DOMAIN FORMATION DURING THE FIRST-ORDER TRANSITION

In a system with enough lateral interaction to cause a first-order phase transition, two phase regions exist separately. During the first-order order-disorder transition between (7×7) and (1×1) on Si (111), and between $c(2 \times 8)$ and (1×1) on Ge (111), for example, reflection electron microscopy and STM studies have shown that each structure exists simultaneously by forming separate domains.[21,23,29,30,44] In the phase transition from InAs-(2×4) to (4×2), As desorption is expected to form desorbed domains in (2×4) structures.

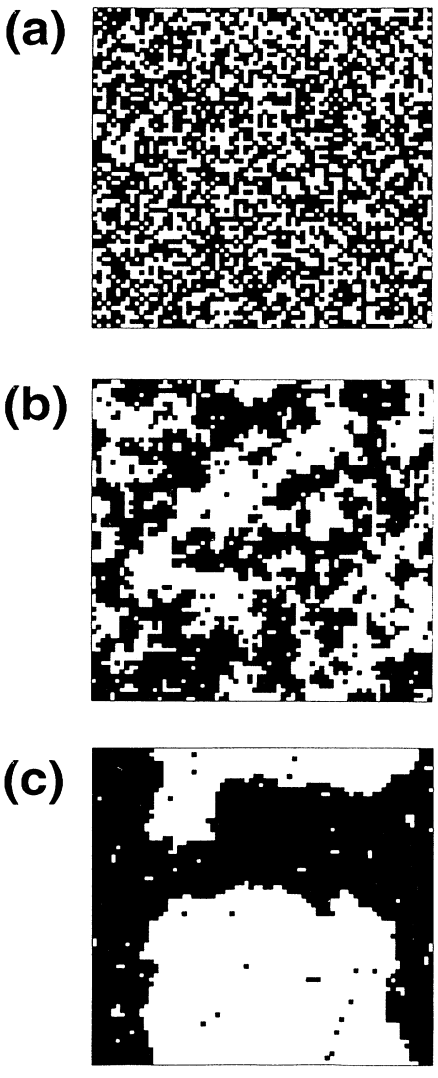

FIG. 14. Calculated As unit distribution on surfaces with a coverage of 0.5 in the transition from As-covered to In-exposed surfaces with (a) E_s=2.5 eV, E_i=0.0 eV, (b) E_s=2.3 eV, E_i=0.1 eV, and (c) E_s=2.18 eV, E_i=0.16 eV. The black domains correspond to As-covered sites and the white domains correspond to In-exposed sites.

Figure 14 shows the calculated As-unit distribution on the surfaces at a coverage of 0.5 in the transition from As covered to In exposed surfaces for different values of E_i. It shows that with small lateral interaction energy, the desorption occurs individually, but in the case of first-order phase transition with strong lateral interaction, the desorption occurs with the formation of exposed In domains. The room-temperature STM study in the previous section indicates that the desorption actually occurs by forming domains [Fig. 12(b)]. In this subsection, we describe *in situ* dynamic observation of first-order phase transitions performed using STM (Ref. 45) and SEM-MBE apparatus.[46] Scanning tunneling microscopy has better atomic resolution but is incapable of observation with As flux. On the other hand, SEM-MBE makes it possible to observe the phase transition with As flux supplied on the surface, but has lower resolution.

A. High-temperature STM observation of GaAs (001) surface

We started by observing a GaAs (001) surface at a high temperature with the STM apparatus. The sample was heated in steps of about 20 °C. Stable (2×4) structures were observed up to 460 °C. Step motion was observed on the GaAs (001) surface after the (2×4) structure had disappeared at 480 °C. Figure 15 shows sequentially obtained STM images at this temperature. Figure 15(b) was obtained 18 sec after 15(a). From the positions of a surface dust particle, the thermal drift was estimated to be less than 2 nm in 18 seconds. Therefore, these two images correspond to almost the same area on the surface.

Unlike Fig. 13(a), no stable dimer-vacancy row structure was observed at this temperature. Each image contains monomolecular steps (A in the figure) and dark regions (B), extending along the $[\bar{1}10]$ direction. Since As desorption from the surface begins to occur at around this sample temperature, the dark regions were probably formed by the desorption of As atoms. The arrows labeled C indicate a weak periodicity along the $[1\bar{1}0]$ direction. The distance between two arrows is 1.2 nm, showing threefold reconstruction, i.e., a (3×1) structure. However, the image does not show a clear atomic structure. The uniformity of the (3×1) structure, the steps, and the dark regions is quite low. This is consistent with the room-temperature STM observation that the (2×4) structure is disordered by As desorption. The shapes of the steps and dark regions differ between the two images, but their motion has no systematic behavior. With

the As-stabilized condition used in conventional MBE growth, enough As atoms are supplied to compensate for the desorption of As, and stable (2×4) structures are established. The non-uniform step motion we observed in our experiments was caused by low As coverage due to the ultrahigh vacuum in the STM chamber.

When the sample was further heated, a mixture of this disordered (3×1) structure and (1×6) was observed (Fig 16). This Ga-rich (1×6) phase[4] was not observed in the transition at high As pressure. This mixed structure indicates that the transition between these two structures is first order. It corresponds to the mixed pattern between disordered (3×1) and Ga stable (4×2), which was observed in a RHEED study as discussed in Sec. III A.

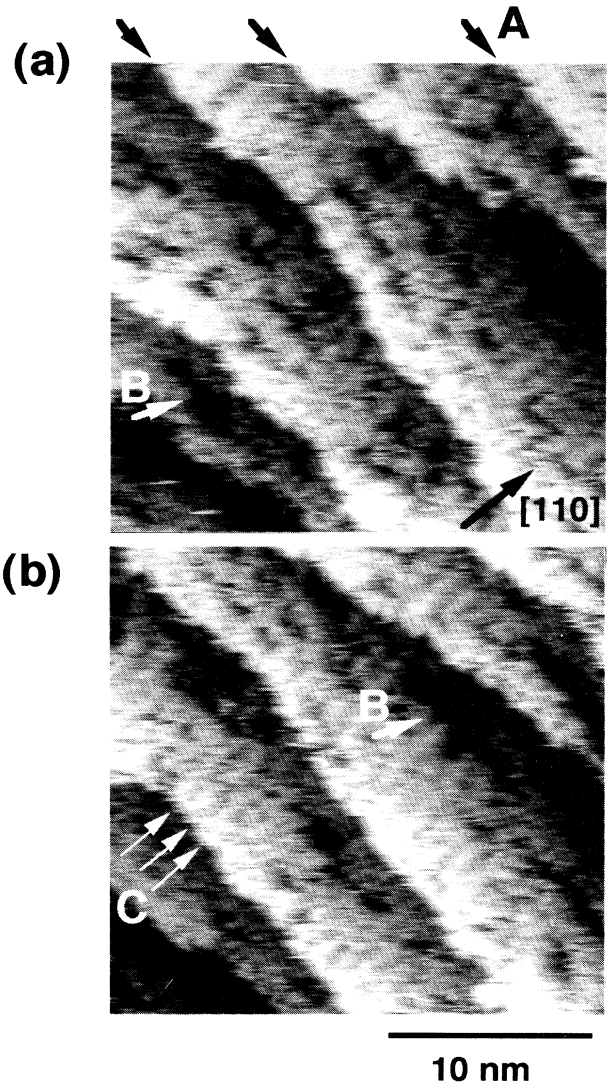

FIG. 15. The STM images of a GaAs (001) surface misoriented 2° toward [110] obtained at 480 °C at 18-s intervals. The image area is 50×50 nm, the bias voltage was −3.5 V, and the tip current was 0.06 nA.

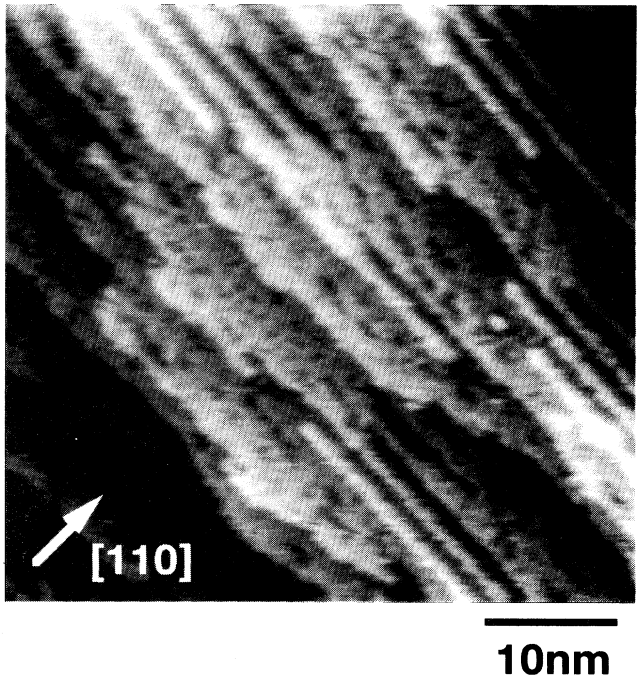

FIG. 16. An STM image of a GaAs (001) disordered (3×1) structure observed at about 500 °C. The surface was misoriented 2° toward [110].

The transition between the disordered (3×1) phase and the Ga stable (1×6) phase is first order, but the transition is continuous, probably due to the finite size effect. We will discuss this point again in Sec. VII.

B. High temperature STM observation of InAs (001) surface

Next, we observed an InAs (001) surface. When the temperature was increased up to 330 °C, the monomolecular steps and kinks were seen to move (Fig. 17). The time interval between the two images is 35 s. The one-molecule-high kinks (*A* in the figure) move in the [1$\bar{1}$0] direction. These images show that steps and kinks move in units of 1.6 nm in the [110] direction. In other words, the kink depths are in units of 4× spacing. This is consistent with the results of static observation of GaAs misoriented surfaces.[47] The resolution of the present images is not high enough to show whether or not the units of the kink and step structures in the [1$\bar{1}$0] direction are 2× spacing. 2× periodicity was observed for the (2×4) structure in terraces even at this temperature, but the periodicity was not clear at the kink edges.

In contrast to the room-temperature observation, a single As-dimer structure [(2×4)-α2] was not obtained. A uniformly wide As-dimer row appeared instead, even just before the transition to (4×2) structures. This is probably because the thermal energy makes the individual As dimers move rapidly from one In exposed site to another.

The change in step structure is due to the surface dif-

fusion of both As and In atoms. On the InAs surface, (2×4) structures can exist stably even at temperatures high enough to cause the diffusion of these atoms. This is probably due to the strength of lateral interactions in the structures. This is consistent with the previous result from room-temperature observations. The (2×4) structure is highly stable against thermal annealing. On the other hand, with GaAs, a disordered STM structure (Fig. 15) was observed because the (2×4) structure is unstable against thermal annealing.

When the temperature of the InAs surface was further increased, we investigated the structural changes occurring when As atoms desorbed. An STM image of an InAs surface obtained at 350 °C (Fig. 18) shows that regions with (4×2) structures (*B* in the figure) appeared surrounded by (2×4) structures (*A*). (The periodic contrast modulation in the vertical direction was caused by the thermal drift.) This result is consistent with the results of Monte Carlo simulation (Fig. 14), and can be explained by strong lateral interaction between surface As units on the InAs (001) surface. Height analysis across the boundary between (2×4) and (4×2) domains shows that the In-exposed (4×2) domain is about 0.1 nm lower than the (2×4) domains. This indicates that the (4×2) domain was actually formed by the desorption of As atoms from the top atomic layer of the (2×4) surface.

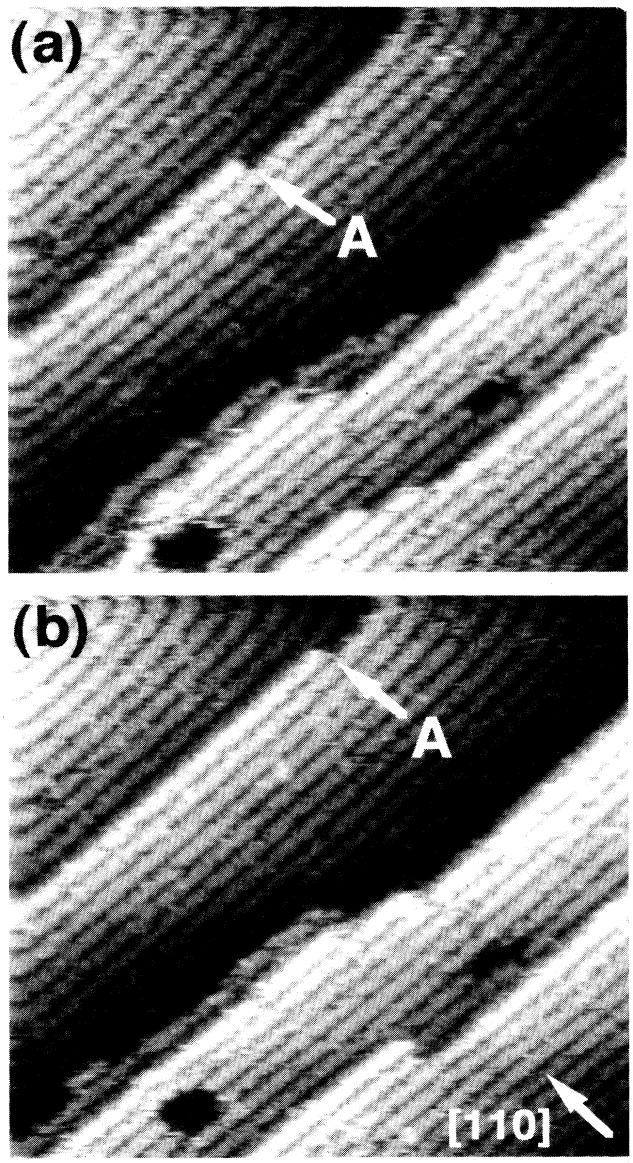

FIG. 17. The STM images of an InAs (001) surface obtained at 330 °C at 35-s intervals. The image area is 50×50 nm, the bias voltage was −3.5 V, and the tip current was 0.08 nA.

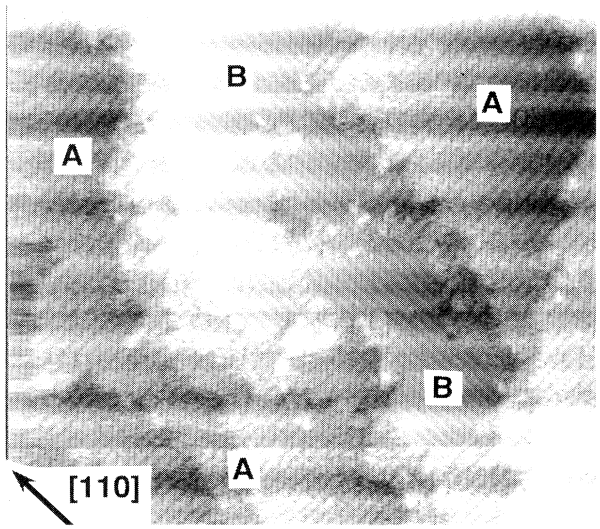

FIG. 18. The STM image of an InAs (001) surface obtained at 350 °C. The image area is 100×100 nm, the bias voltage was −2.0 V, and the tip current was 0.08 nA.

C. *In situ* observation of domain formation by SEM-MBE system

Phase transitions on InAs surfaces are harder to observe directly because they occur reversibly only under group V pressure, i.e., in an MBE chamber. Although the high temperature STM observations in ultrahigh vacuum in the previous sections help us to understand these transitions, they were not performed under thermal equilibrium conditions. We used a newly developed SEM/MBE system, i.e., a high-resolution UHV-SEM apparatus with a liquid nitrogen shroud and effusion cells,[24] which makes it possible to perform SEM observations even when molecular beams are applied to the sample surface. The SEM system directly confirmed that the domain formation predicted by Monte Carlo simulation occurs under the same thermal equilibrium condition as in the RHEED observations.

Figure 19 shows secondary electron (SE) images of an InAs (001) surface 1° misoriented toward the [110] direction obtained when we increased the temperature up to

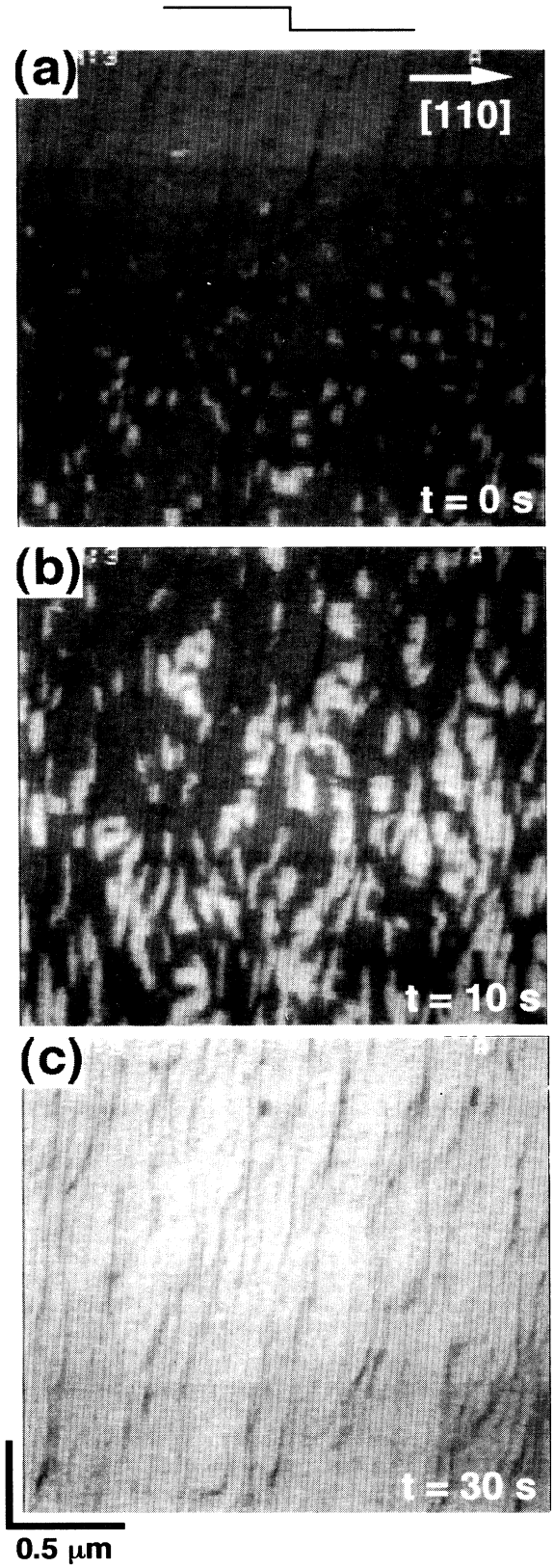

FIG. 19. The SEM images of an InAs 1°-*A* surface during the transition from (2×4) to (4×2) structures. (b) was obtained 10 s after (a), and (c) was obtained 20 s after (b). Steps proceed downward from left to right.

480 °C. A period of ten seconds was necessary for scanning the area. The RHEED pattern showed that the surface structure changed from (2×4) to (4×2) at this temperature. The dark domain thus corresponds to a (2×4) structure, the light domain corresponds to a (4×2) structure, and the growth of (4×2) domains is clearly visible. These results directly indicate that domains are formed during the transition as predicted by the two-dimensional lattice-gas model.

The expected terrace size along the [110] direction, calculated from the misorientation angle of 1°, is 16 nm. However, the size actually observed in Fig. 19 is about 80 nm, showing that the steps bunch together in multistep structures. Step bunching has also been identified by STM observation[48] and SEM observation of growth-interrupted GaAs (001) surfaces,[24] and atomic force microscopy observation of a surface grown by metal-organic chemical-vapor deposition.[49] When about half surface coverage changed to (4×2), the (4×2) domains had an average size of from 20 nm to 100 nm in the [110] direction and from 100 to 500 nm in the [1$\bar{1}$0] direction. The anisotropic shape of these domains is due to their being bounded by the multisteps running in the [1$\bar{1}$0] direction.

VII. INFLUENCE OF SURFACE STEPS ON THE PHASE TRANSITION

In the Monte Carlo simulation, we have assumed that no monomolecular steps are formed on the InAs surface during observation. Next the influence of monomolecular steps on the first-order phase transition was studied by using misoriented substrates.[50] This influence is the so-called finite size effect on the first-order transition. Many theoretical studies have investigated finite size effects on phase transitions, for example, by Monte Carlo simulations and renormalization-group treatments.[37] In general, a phase transition can occur in a system with infinite degrees of freedom, but in a finite system the physical quantity has no singularity as a function of temperature (or other parameters in general). The metastability associated with the first-order phase transition is broken by making the system size finite. For sufficiently large systems, the quantity has an abrupt dependence at the singular point and this abruptness increases when the system size increases. This influence of system size on the phase transition is theoretically well known, and has also been studied experimentally for a number of physical systems. For example, finite size effects on semiconductor surfaces were reported for an irreversible transition from Si(111)-(2×1) to (7×7) according to measurements of LEED patterns and surface conductivity,[15] and for the transition between Si(111)-(7×7) and (1×1) according to reflection electron microscopy[29] and STM measurements.[21]

Here, we discuss the finite size effects on the first-order phase transition of InAs (001) surfaces by using misoriented surfaces. Periodic monomolecular steps or multisteps are formed on the misoriented surface, and these steps can cut off or reduce the lateral interaction across the steps between surface atoms. This made the system

size finite along the misorientation direction. By observing the effects of this misorientation on phase transitions, we can study the finite size effects experimentally. This makes it possible to prove the existence of lateral interaction, which was assumed in the lattice-gas model proposed in the previous sections.

A. RHEED measurements

Three types of undoped n-type InAs were used as substrates. One was exactly oriented (001), one was misoriented 2° toward the [110] direction (called the A surface), and the other was misoriented 1° or 2° toward the $[1\bar{1}0]$ direction (the B surface). A (001) InAs 2° misoriented surface has an average terrace width of about 8 nm. Because the two-dimensional primitive cells of this surface form a square lattice with a lattice constant of 0.4 nm, 20 arsenic atoms lie in a row along the misorientation direction if no step bunching occurs on the surface. Even if we assume that As is desorbed and adsorbed as single atoms, the system size along the misorientation direction is limited to 20 units. This means that the existence of periodic monomolecular steps makes the system size finite.

The variation of RHEED specular beam intensity as a function of substrate temperature exhibits 10 °C of hysteresis for incident azimuths of both [110] and $[1\bar{1}0]$ for a correctly oriented surface. Figure 20 shows the results obtained with 2° misoriented surfaces. The hysteresis of the A surface exhibits a similar width as that of an exactly oriented surface, but that of the B surface, 3.5 °C, is smaller. On a 1° misoriented substrate, the hysteresis width of B surface was 5.3 °C. Therefore, the hysteresis width decreases with increasing misorientation angle. A decrease of hysteresis width means a drop of metastability associated with the first-order phase transition. This experimental result shows that the expected finite size effect was observed on the B surface, but was insignificant on the A surface.

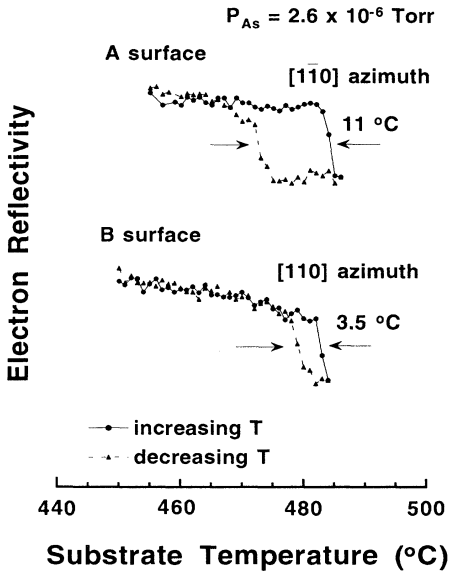

FIG. 20. Reflection high-energy electron diffraction specular beam intensity as a function of substrate temperature for InAs (001) surfaces misoriented toward the [110] (A surface) and the $[1\bar{1}0]$ (B surface) directions. An As flux of 2.6×10^{-6} Torr was supplied during the measurement, and $[1\bar{1}0]$ and [110] azimuths were used for the A and B surfaces, respectively.

B. Monte Carlo simulations for misoriented surfaces

To explain this finite size effect due to the surface misorientation, we performed a Monte Carlo simulation for an InAs misoriented surface, using the following boundary conditions at the step edge: An As unit on one side of the step edge has no interaction across the step edge, while an As unit on the other side of the step edge interacts with an energy of E_i across the step edge, regardless of the existence of the As unit on the opposite side [Fig. 21(a)]. Figure 21(b) shows the calculated hysteresis width with several terrace widths for E_s=2.18 eV and E_i=0.16 eV. As expected from the experimental results, the hysteresis width decreases as the terrace width

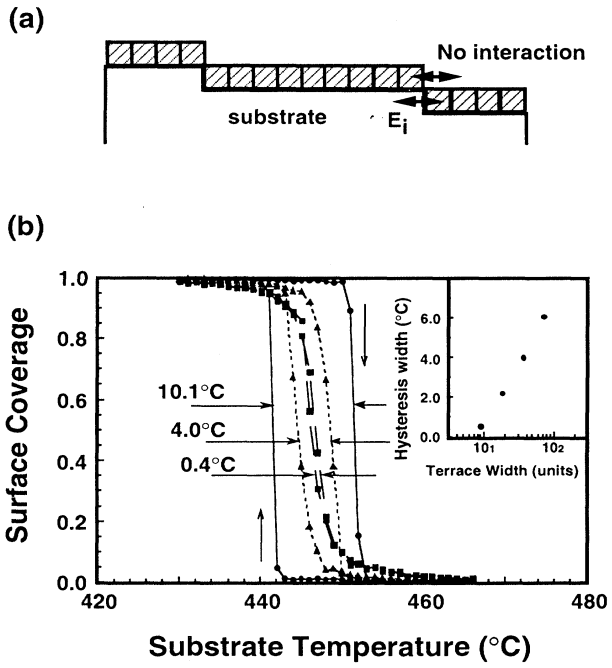

FIG. 21. (a) The boundary condition used in the simulation of misoriented surfaces. (b) The calculated As coverage as a function of substrate temperature for misoriented surfaces with different terrace widths. The solid curve corresponds to an exactly oriented surface, and the dotted and dashed curves correspond to misoriented surfaces with terrace widths of 36 and 9 units, respectively. Inset: Resulting plot of hysteresis vs terrace width.

decreases. This finite size effect on the first-order transition is consistent with our experimental results. For misoriented surfaces, the As unit at the step edge has no interaction across the step. Therefore, the unit has less activation energy and can desorb from the surface more easily than those in the terraces. If this happens, the metastability resulting from the strong As-As interaction is broken and the hysteresis width decreases. This gives a physical explanation of the phenomenon.

Figure 22 shows the simulated change of surface structure during the transition from (2×4) to (4×2). The result clearly indicates that As desorption occurs from step edges, thereby reducing the metastability of the system.

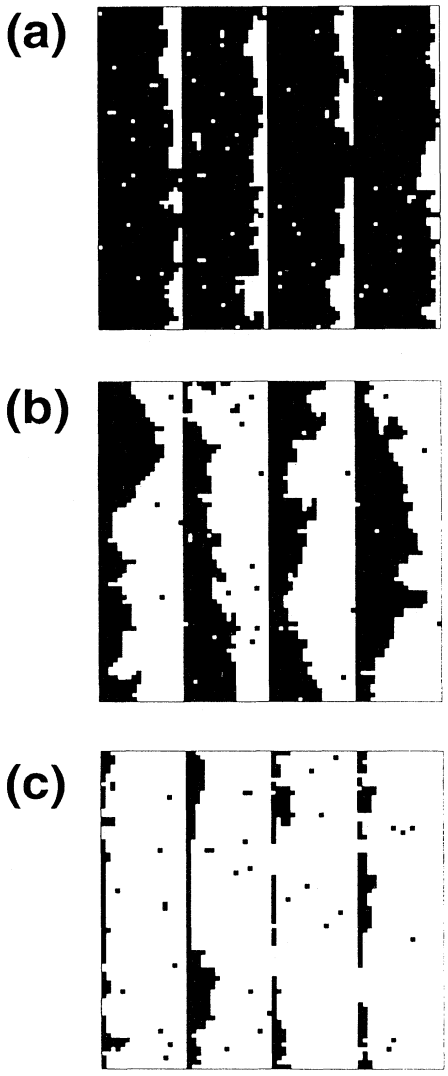

FIG. 22. Calculated As-unit distribution on a misoriented surface with a terrace size of 18 As units during the transition at temperatures of (a) 446 °C, (b) 448 °C, and (c) 449 °C for E_s=2.18 eV and E_i=0.16 eV. The black domains correspond to As-covered sites and the white domains correspond to In-exposed sites.

C. The origin of anisotropic behavior

In our experimental results, the finite size effect was confirmed only on a B surface. There are three ways to explain the difference between A and B surfaces. One is the anisotropic lateral interaction between surface species.[50] The experimental results can show that the interaction is stronger in the [1$\bar{1}$0] direction than in the [110] direction. Here, we consider the typical results obtained in simulations with E_i=0.03 eV in the [110] direction and E_i=0.15 eV in the [1$\bar{1}$0] direction. In this simulation, we assumed a terrace width of 18, which corresponds to the average number of As atoms in a row along the misorientation direction on a 2° misoriented surface. The calculated hysteresis widths for a correctly oriented surface, an A surface and a B surface were 8.7 °C, 4.9 °C, and 0.6 °C. These values do not exactly match the experimental results in that there was no reduction in the hysteresis width for an A surface. Therefore, there must be another reason besides anisotropy in lateral interactions.

The second is the role of steps. It is well known that the finite size effect on the phase transition is very sensitive to the boundary conditions.[37] In the simulation, we simply used the boundary condition that the lateral interaction is terminated at the step edge. The boundary is a *free edge* at the upper side of the step and a *fixed edge* at the lower side of the step. This assumption is too simple. There must be some change in the vertical interaction, E_s, at the step edge and the lateral interaction may not be perfectly terminated at the step edge. If we assume that E_s is higher at the step edge, the desorption of As is not largely influenced by the step edge. This suggests that an As atom at the step edge on an A surface is as energetically stable as those in the terraces.

The third one is step bunching. It has been reported that a GaAs (001) surface has a multistep structure caused by growth[49] and also by growth interruption.[24,48] If step bunching occurs on InAs misoriented surfaces, the finite size effect is not significant. In fact, the SEM image in Sec. VI C (Fig. 19) shows that the steps are bunched on the A surface. We discuss this point in more detail in the following sections based on *in situ* high-temperature observations made with a STM and a combined SEM-MBE system.

D. STM observation of As desorption from step edge

Figure 23 shows STM images obtained during the transition from (2×4) to (4×2) in a region with high step density. Figure 23(b) was obtained 35 s after (a). Some of the (2×4) regions observed in (a) (for example, the regions indicated by arrows in the figure) disappeared in (b). This indicates that As desorption occurred and reconstruction changed the configuration to (4×2) in that region. It is clearly seen that the transition preferentially occurs from step edges parallel to [110]. On the other hand, we have not observed As desorption from step edges parallel to the [1$\bar{1}$0] direction. This difference in the role of steps on the As desorption is important

for discussing the anisotropic behavior of the finite size effect.

E. SEM observation for misoriented surfaces

The STM observation indicated that As desorption does not begin from A steps (monomolecular steps parallel to $[1\bar{1}0]$) but from B step (monomolecular steps parallel to $[110]$). This is one reason why the finite size effect was insignificant on an A surface. However, there are still two questions. One is the role of steps during the As adsorption and the other is the effect from the step bunching. The SEM observation in Sec. VI C shows that the steps are bunched both for (2×4) and (4×2) on an A surface. This is another reason why the finite size effect was insignificant on an A surface. The fact that the finite size effect was observed on surface B indicates that multisteps did not form on at least one of the (2×4) and (4×2) surfaces. The SEM observation clarified these two questions.

Figure 24 shows SE images of an InAs (001) A surface with 1° misorientation at about 470 °C obtained when the sample was cooled and underwent transition from (4×2) to (2×4). This transition temperature, about

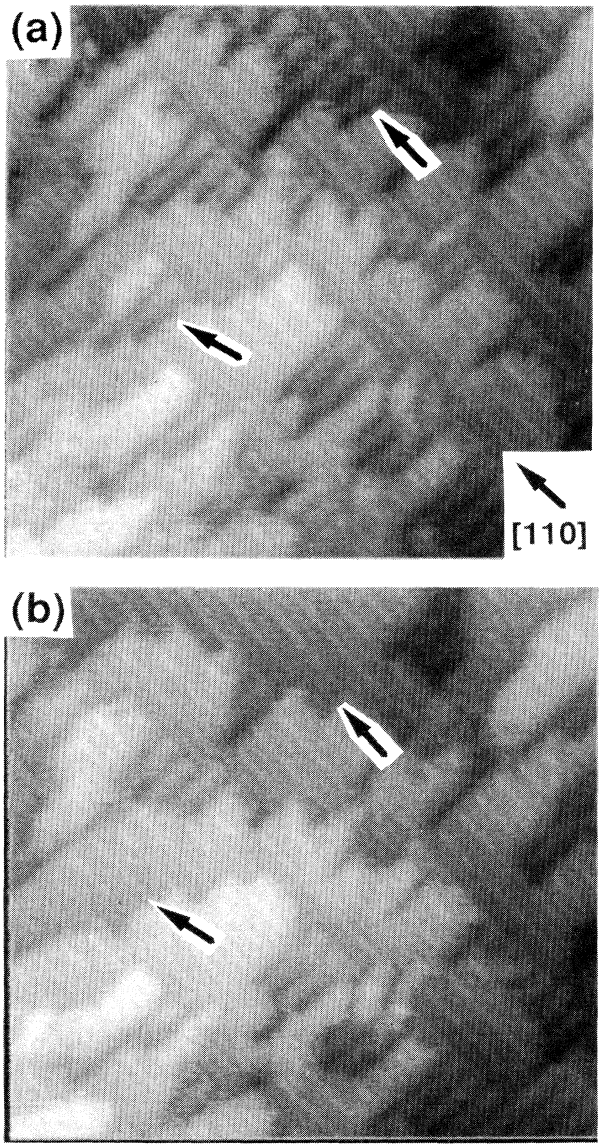

FIG. 23. The STM images of an InAs (001) surface obtained at 350 °C at an interval of 35 s. The image area is 40×40 nm, the bias voltage was −2.5 V, and the tip current was 0.1 nA.

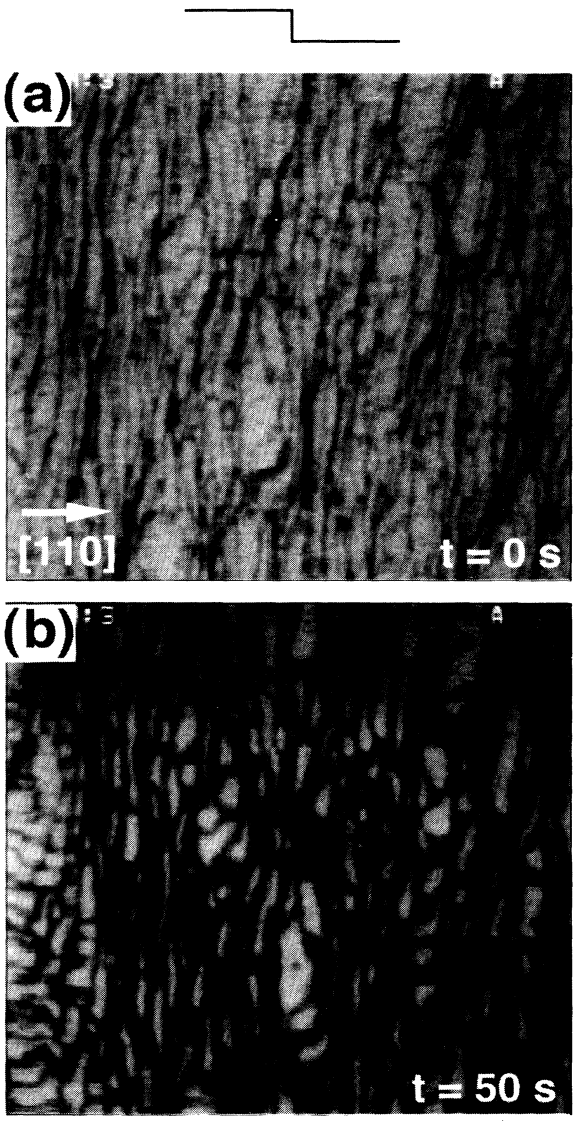

FIG. 24. Secondary electron image of an InAs (001) surface during the transition from a (4×2) to a (2×4) surface. (a) was obtained just after the transition began, and (b) was obtained 50 s later. The image size is 2.3 μm (horizontal) × 2.9 μm (vertical).

10 °C lower than that from (2×4) to (4×2), has similar hysteresis width to the results of RHEED observations. The role of monomolecular steps during the transition from (4×2) to (2×4) differs from that from (2×4) to (4×2). At the beginning of the transition from (4×2), the steps are darker than the terraces shown in Fig. 24(a). This enhanced contrast at the multisteps indicates that the As atoms preferentially adsorb at the step edge.[46] [This was not observed for the transition from (2×4) to (4×2); the steps in Fig. 19(a) are not brighter than the terraces but are rather darker, indicating that the step edge does not act as the desorption site.] Growth of (2×4) domains from the step edge was observed when the temperature was decreased to 2 or 3 °C below the temperature at which the contrast enhancement was observed in Fig. 24(a).

Because the As atoms do not desorb from the step edge on an A surface, the As atoms at the higher side of the step edge must be as energetically stable as those on the terraces. If the As atoms have no lateral interaction across the step edge and have the same vertical interaction with underlying In atoms as those on the terraces, the As desorption would begin at the step edge as expected in the Monte Carlo simulations. The experimental result shows that this is not the case of an A surface. On the other hand, adsorption begins from the step edge as would be expected from the lattice-gas model. The role of step edges during transition, therefore, differs between As desorption and adsorption.

Next, we compared the formation of multisteps on 2°-A and 2°-B surfaces. Figure 25 shows SE images of (2×4) and (4×2) surfaces of a 2°-A surface. We used a slower scan with a scan time of 70 s to increase the image resolution. The SE intensity is higher in the (4×2) domains than in the (2×4) domains, as mentioned already, but the brightness and the grayscale of the image were adjusted to make it easier to see the steps. A multistep structure was observed for both (2×4) and (4×2) surfaces. The average distance between two visible steps is about 60 nm, which is smaller than on the 1°-A surface, for both reconstructions. The steps are clearer for (4×2) than for (2×4), indicating weaker step bunching with the latter than the former. However, the step structure is not significantly different between these two surface reconstructions. The images were both obtained after the sample temperature had been repeatedly raised and lowered. It was confirmed that the clear multistep structure was not observed just after the As decapped layer was removed. The commonly observed multistep structure in Fig. 25 was initially formed after the first transition from (2×4) to (4×2), and maintained even after the transition from (4×2) to (2×4).

On the other hand, with a 2°-B surface, the step structure depends strongly on the surface reconstruction. Figure 26 shows SE images of (2×4) and (4×2) surface reconstructions. Although a bunched step structure is seen in the (4×2) surface, no steps were observed in the (2×4) surface, even at the highest resolution. This result was reproducibly observed when we repeatedly raised and lowered the sample temperature. This indicates that multisteps do not form with a (2×4) structure, and that step bunching and debunching occur during the transitions from (2×4) to (4×2) and from (4×2) to (2×4) structures, respectively. This reconstruction-dependent step bunching was also recently reported for a GaAs (001) surface.[51] The reason why single monomolecular steps were not resolved for the (2×4) structure on 2°-A surfaces is probably because the distance between two neighboring steps, 8 nm in this case, is too small and the single step fluctuates as indicated by RHEED (Ref. 52) and STM (Ref. 47) observations.

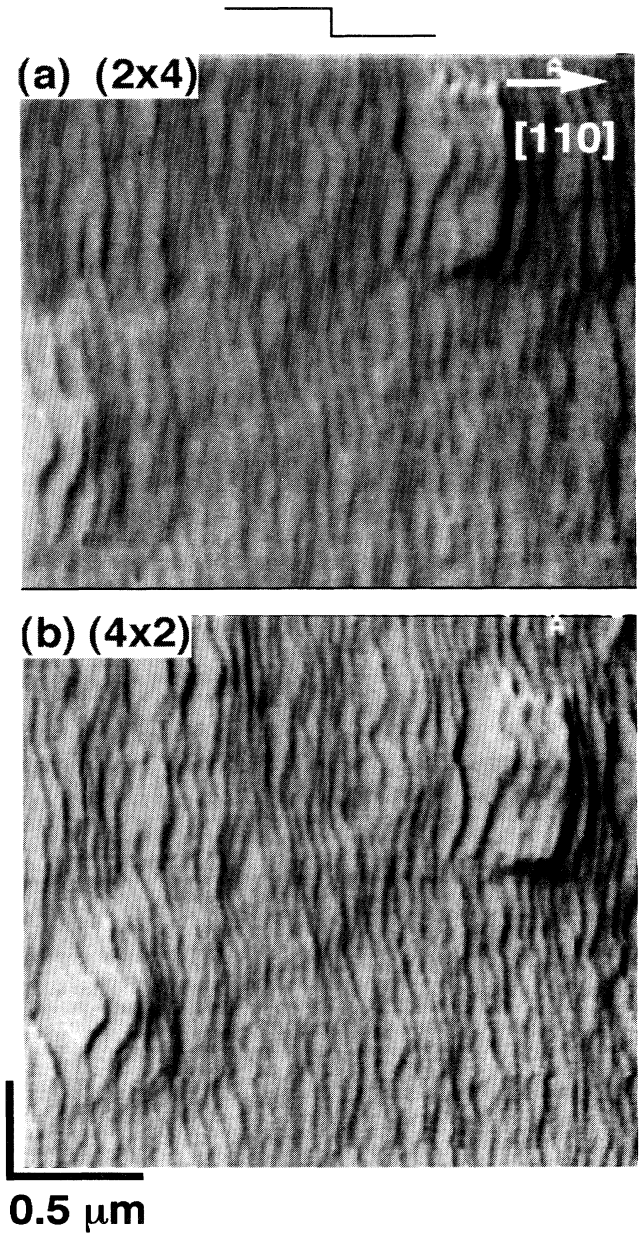

FIG. 25. The SEM images of an InAs 2°-A surface with (a) (2×4) and (b) (4×2) structures. Steps proceed downward from left to right.

Therefore, a multistep structure was formed both on A surfaces and B surfaces with (4×2) structure, but only on A surfaces with (2×4) surface. This is one reason why the finite size effect is more significant for B surfaces than A surfaces. The small hysteresis width of B surfaces is mainly due to As desorption from the edges of B steps. For adsorption, the role of steps is not marked because a wide terrace is formed by step bunching, although adsorption occurs from the step edge both for A surfaces and B surfaces.

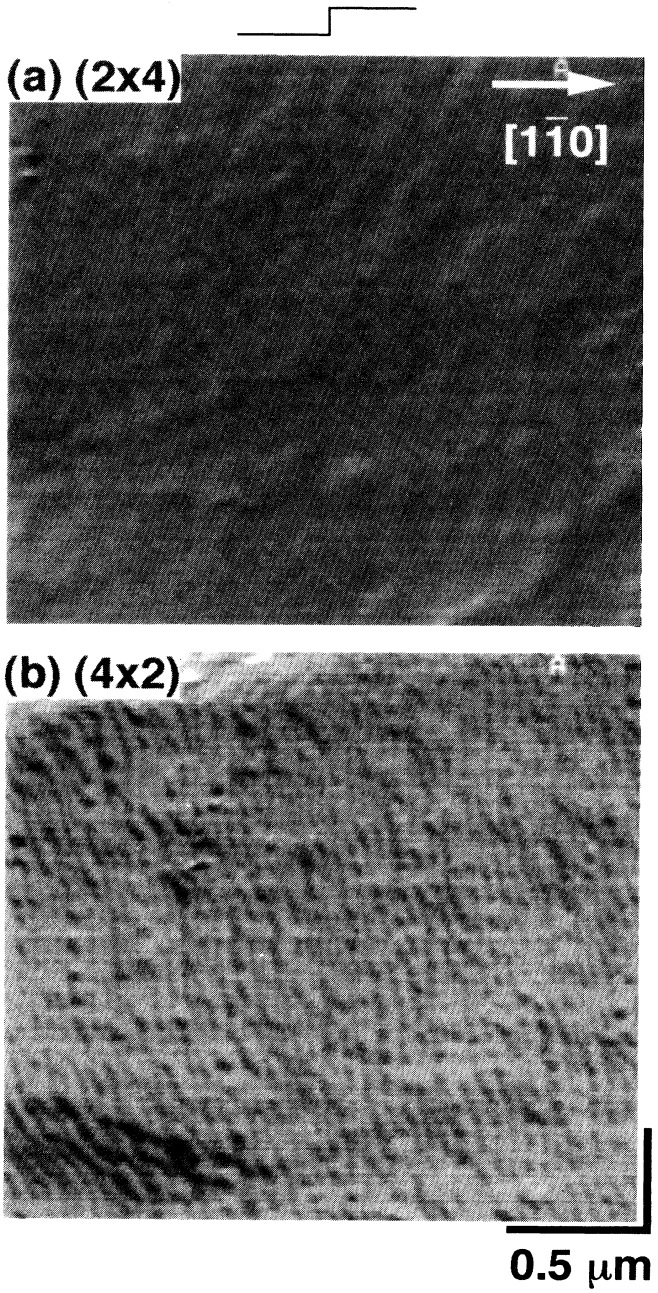

FIG. 26. The SEM images of an InAs 2°-B surface with (a) (2×4) and (b) (4×2) structures. Steps proceed downward from right to left.

F. Transition between (3×1) and (4×2) on GaAs (001)

We must mention here the finite size effect on the transition between disorder (3×1) and Ga-stable (4×2) [or (1×6) without As pressure] surfaces. Our RHEED and STM studies showed that the mixed pattern can be observed during the transition. This means that the transition is first order. However, the transition was continuous, as mentioned in Sec. III A. This is probably due to the finite size effect which deteriorates the metastability of the system as shown in the previous sections. This is actually observed in the order-disorder transition between (1×1) and (7×7) on a Si (111) surface. The electron diffraction intensity changes continuously during the transition,[21,29,30] but the other direct observation methods show that each domain is formed during the transition. The growth of each domain from the surface monatomic steps was observed, indicating the finite size effect due to the steps.

In the case of InAs (001), even with the influence of the steps, the RHEED intensity change shows some hysteresis. This indicates the influence is more significant with transitions on Si (111) than those on InAs (001). The reason is probably the kinetics which limit the transition. The Si (111) order-disorder transition is limited by surface diffusion. The time constant of the diffusion is very small compared with the time scale for the observation. Hence, no hysteresis was observed, and the transition is continuous for Si (111). On the other hand for InAs (001), the transition is limited by desorption and adsorption. These processes have comparable time constants with the observation time. Therefore, the transition still has small hysteresis even with the influence of the steps as shown in the simulation. The reason why the transition between disorder (3×1) and Ga-stable (4×2) [or (1×6)] surfaces is continuous can be the same as for the transition on Si (111), i.e., the transition is not limited by adsorption and desorption but limited by the surface diffusion of As and Ga atoms.

VIII. CONCLUSION

We have studied the phase transition between As-stable (2×4) and In/Ga-stable (4×2) structures on InAs and GaAs (001) surfaces using RHEED, STM, SEM, and Monte Carlo simulation. There is a large difference between InAs (001) and GaAs (001) surfaces in the transition, which is discontinuous for InAs (001) but continuous for GaAs (001). The discontinuous transition on InAs (001) was shown to be caused by strong lateral interaction between surface species. The difference between InAs and GaAs was explained by the difference in the transition temperature, T_t, and the atomic structure of the (2×4) surface. We also discussed the influence of surface atomic steps on the phase transition on InAs (001). This influence largely depends on the misorientation direction. The dependence was explained in terms of step bunching and the role of steps in the desorption and adsorption of As atoms.

ACKNOWLEDGMENTS

We are indebted to Professor Bruce Joyce, Kenji Shiraishi, Yasuhiro Tokura, Makoto Kasu, and Hibino Hiroki for their valuable discussions, and Yoshikazu Homma for his helpful support on the SEM observations. We thank Tatsuya Kimura for his continuous encouragement during this work.

[1] *Molecular Beam Epitaxy and Heterostructures*, edited by L.L. Chang and K. Ploog (Nijhoff, Dordrecht, 1985).
[2] *The Technology and Physics of Molecular Beam Epitaxy*, edited by E. H. C. Parker (Plenum, New York, 1985).
[3] A. Y. Cho, J. Appl. Phys. **42**, 2074 (1971).
[4] P. Drathen, W. Ranke, and K. Jacobi, Surf. Sci. **77**, L162 (1978).
[5] J. H. Neave and B. A. Joyce, J. Cryst. Growth **44**, 387 (1978).
[6] J. Massies, P. Etienne, F. Dezaly, and N. T. Linh, Surf. Sci. **99**, 121 (1980).
[7] C. Deparis and J. Massies, J. Cryst. Growth **108**, 157 (1991).
[8] M. D. Pashley, K. W. Haberern, W. Friday, J. M. Woodall, and P. D. Kirchner, Phys. Rev. Lett. **60**, 2176 (1988).
[9] D. K. Biegelsen, R. D. Bringans, J. E. Northrup, and L.-E. Swartz, Phys. Rev. B **41**, 5701 (1990).
[10] H. H. Farrell and C. J. Palmstrøm, J. Vac. Sci. Technol. B **8**, 903 (1990).
[11] D. J. Chadi, J. Vac. Sci. Technol. A **5**, 834 (1987).
[12] T. Ohno, Phys. Rev. Lett. **70**, 631 (1993).
[13] J. E. Northrup and S. Froyen, Phys. Rev. Lett. **71**, 2276 (1993).
[14] See, for example, B. N. J. Persson, Surf. Sci. Rep. **15**, 1 (1992).
[15] W. Mönch, Surf. Sci. **63**, 79 (1977).
[16] P. A. Bennett and M. W. Webb, Surf. Sci. **104**, 74 (1981).
[17] R. J. Phaneuf and M. B. Webb, Surf. Sci. **164**, 167 (1985); J. Arts, A.-J. Hoeven, and P. K. Larsen, Phys. Rev. B **38**, 3925 (1988).
[18] M. D. Pashley and K. W. Haberern, Phys. Rev. Lett. **67**, 2697 (1991).
[19] H. Yamaguchi and Y. Horikoshi, Phys. Rev. B **44**, 5897 (1991).
[20] S. P. Kowalczyk, D. L. Miller, J. R. Waldrop, P. G. Newman, and R. W. Grant, J. Vac. Sci. Technol. **19**, 255 (1981).
[21] S. Kitamura, T. Sato, and M. Iwatsuki, Nature **351**, 215 (1991).
[22] Y. Homma, M. Tomita, and T. Hayashi, Ultramicroscopy **52**, 187 (1993).
[23] Y. Homma, M. Suzuki, and M. Tomita, Appl. Phys. Lett. **62**, 3276 (1993).
[24] Y. Homma, J. Osaka, and N. Inoue, Jpn. J. Appl. Phys. **52**, 187 (1993).
[25] H. Yamaguchi and Y. Horikoshi, Phys. Rev. B **45**, 1511 (1992).
[26] J. M. Moison, C. Guille, and M. Bensoussan, Phys. Rev. Lett. **58**, 2555 (1987).
[27] Y. Horikoshi, H. Yamaguchi, F. Briones, and M. Kawashima, J. Cryst. Growth **105**, 326 (1990).
[28] L. Leprince, F. Houzay, and J. M. Moison, Phys. Rev. B **48**, 14 683 (1993).
[29] N. Osakabe, Y. Tanishiro, K. Yagi, and G. Honjo, Surf. Sci. **109**, 353 (1981).
[30] W. Telieps and E. Bauer, Surf. Sci. **162**, 163 (1985).
[31] H. Yamaguchi and Y. Horikoshi, Appl. Phys. Lett. **64**, 2572 (1994).
[32] *Adsorption on Metal Surfaces*, edited by J. Bénard (Elsevier, New York, 1983), Chap. 3.
[33] V. Bressler-Hill, M. K. Pond, R. Moboudian, G. A. D. Briggs, P. M. Petroff, and W. H. Weinberg, J. Vac. Sci. Technol. B **10**, 1881 (1992).
[34] J. Zhou, Q. Xue, H. Chaya, T. Hashizume, and T. Sakurai, Appl. Phys. Lett. **64**, 583 (1994).
[35] The lateral interaction does not need to be an As-As interaction on the (2×4) surface, but can be an In-In interaction on the (4×2) surface, or any formation energy of surface reconstruction per one pair of desorption/adsorption units.
[36] L. Onsager, Phys. Rev. **65**, 117 (1944).
[37] See, for example, *Monte Carlo Methods in Statistical Physics*, 2nd ed., edited by K. Binder (Springer-Verlag, Berlin, 1986).
[38] G. H. Gilmer and P. Bennema, J. Appl. Phys. **43**, 1347 (1972).
[39] S. Clark and D. D. Vvedensky, Phys. Rev. Lett. **58**, 2235 (1987).
[40] P. A. Maksym, Semicond. Sci. Technol. **3**, 594 (1988).
[41] J. E. Northrup and S. Froyen, Phys. Rev. B **50**, 2015 (1994).
[42] H. Yamaguchi and Y. Horikoshi, Jpn. J. Appl. Phys. **33**, L1423 (1994).
[43] T. Hashizume, Q. K. Xue, J. Zhou, A. Ichimiya, and T. Sakurai, Phys. Rev. Lett. **73**, 2208 (1994).
[44] R. M. Feenstra, A. J. Slavin, G. A. Held, and M. A. Lutz, Phys. Rev. Lett. **66**, 3257 (1991).
[45] H. Yamaguchi and Y. Horikoshi, Phys. Rev. B **48**, 2807 (1993); Jpn. J. Appl. Phys. **33**, 716 (1994).
[46] H. Yamaguchi, Y. Homma, and Y. Horikoshi, Appl. Surf. Sci. **82/83**, 223 (1994).
[47] M. D. Pashley, K. W. Haberern, and J. M. Gaines, Appl. Phys. Lett. **58**, 406 (1991).
[48] T. Ide, A. Yamashita, and T. Mizutani, Phys. Rev. B **46**, 1905 (1992).
[49] M. Kasu and T. Fukui, Jpn. J. Appl. Phys. **31**, L864 (1992).
[50] H. Yamaguchi and Y. Horikoshi, Phys. Rev. Lett. **70**, 1299 (1993).
[51] S. L. Skala, S. T. Chou, K.-Y. Cheng, J. R. Tucker, and J. W. Lyding, Appl. Phys. Lett. **65**, 722 (1994).
[52] P. R. Pukite, G. S. Petrich, S. Batra, and P. I. Cohen, J. Cryst. Growth **95**, 269 (1989).

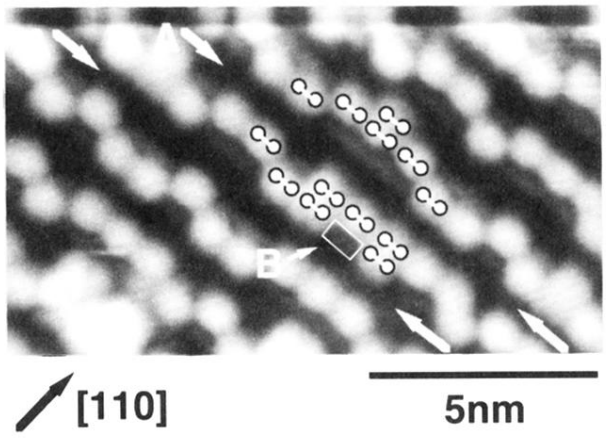

FIG. 11. The STM image of an InAs (001) (2×4) surface annealed at 340 °C. The sample bias voltage was −2.0 V and the tip current was 0.10 nA. The arrows labeled "*A*" show the dimer-vacancy rows, and As dimers are depicted on the image following the expected model. The arrow labeled "*B*" indicates the exposed In layer, one atomic layer below the top As layer.

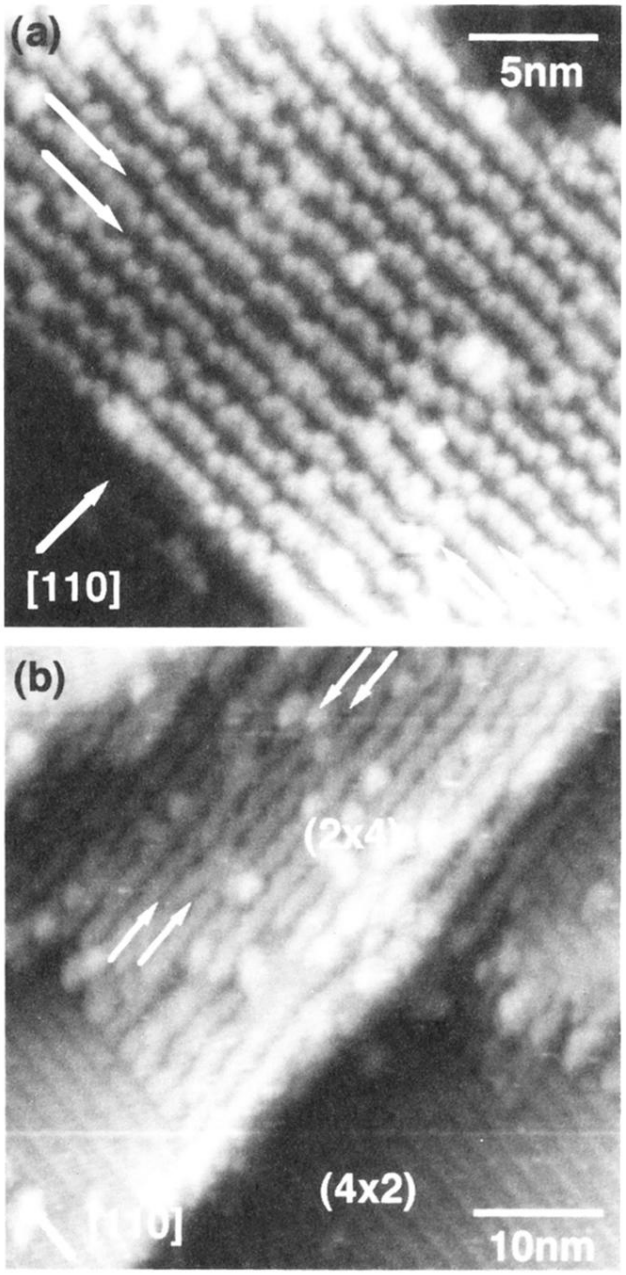

FIG. 12. The STM images of InAs (001) surfaces annealed at (a) 340 °C and (b) 370 °C. These images were obtained with bias voltages of −2.4 V and −3.0 V and with tip current of 0.10 nA and 0.08 nA, respectively. The arrows indicate As dimer-vacancy rows.

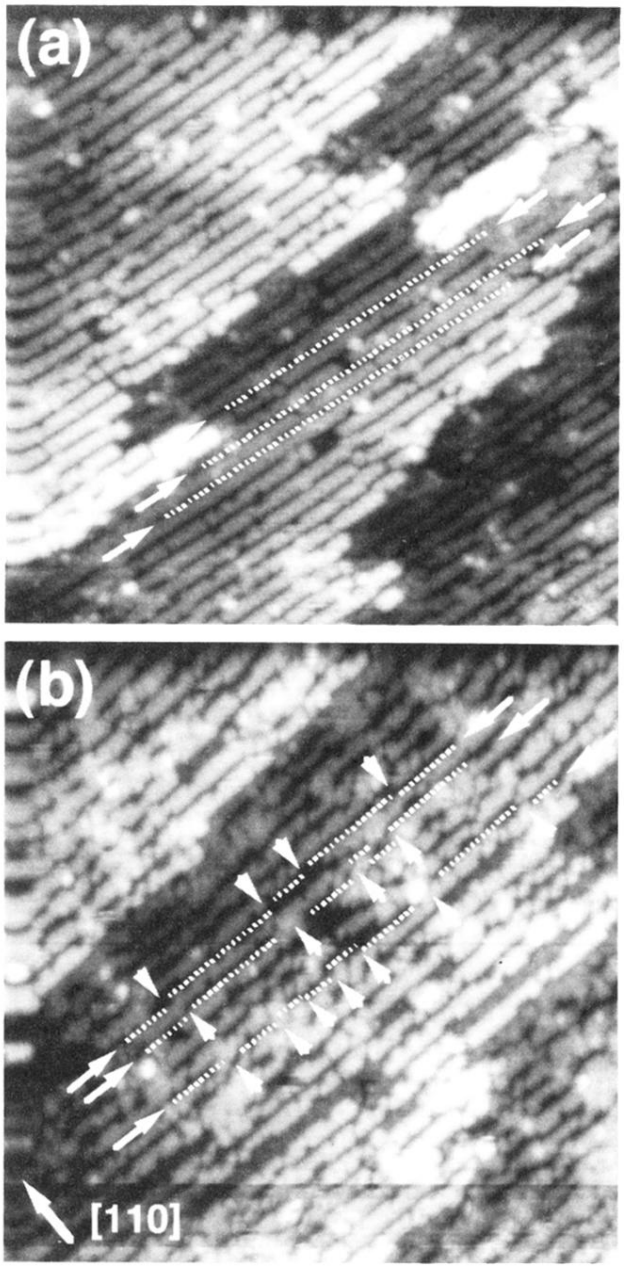

FIG. 13. The STM images of GaAs (001) surfaces (a) just after the growth and (b) after annealing at 490 °C for 1 min. The arrows indicate As dimer-vacancy rows, which are straight in (a) but include some kinks in (b).

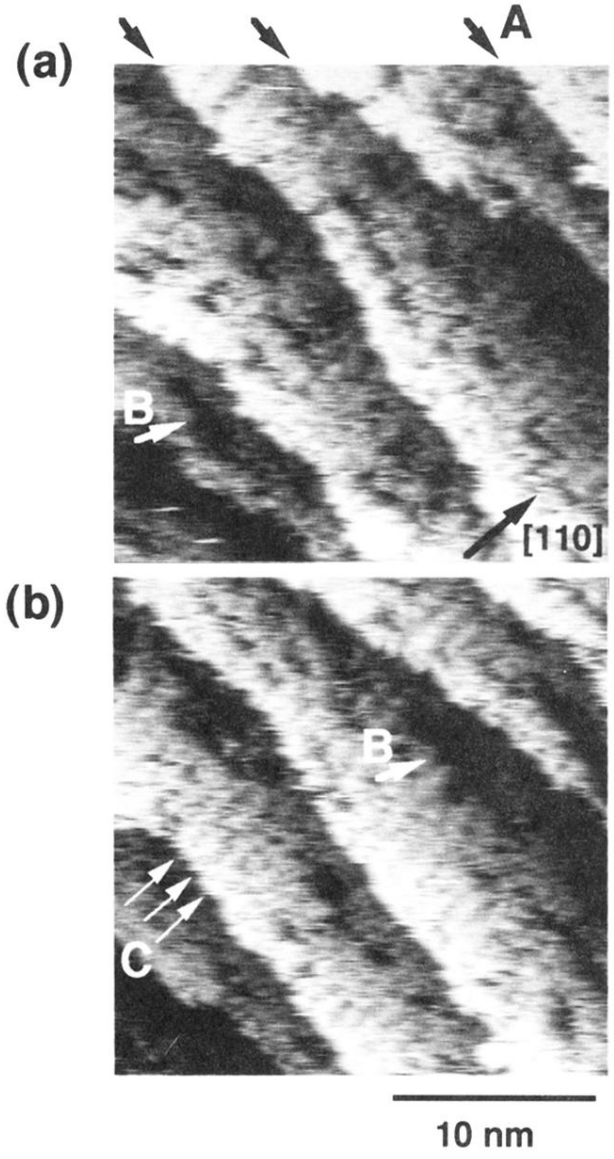

FIG. 15. The STM images of a GaAs (001) surface misoriented 2° toward [110] obtained at 480 °C at 18-s intervals. The image area is 50×50 nm, the bias voltage was −3.5 V, and the tip current was 0.06 nA.

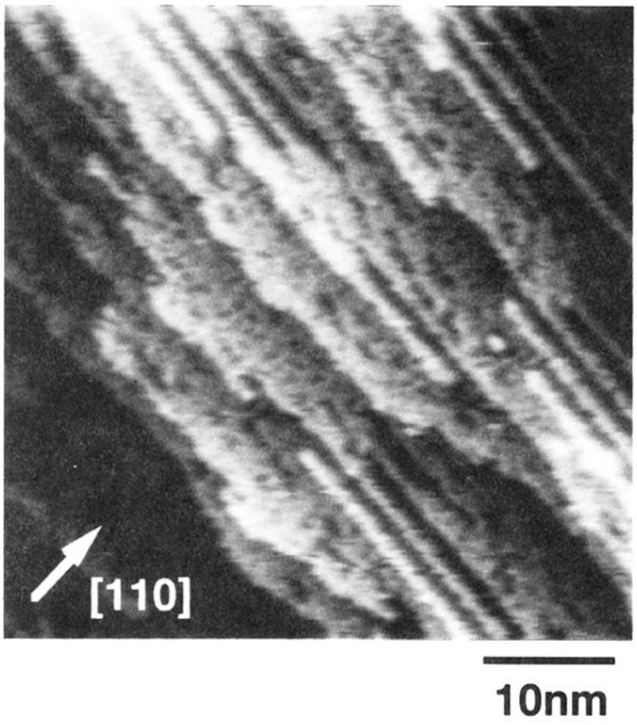

FIG. 16. An STM image of a GaAs (001) disordered (3×1) structure observed at about 500 °C. The surface was misoriented 2° toward [110].

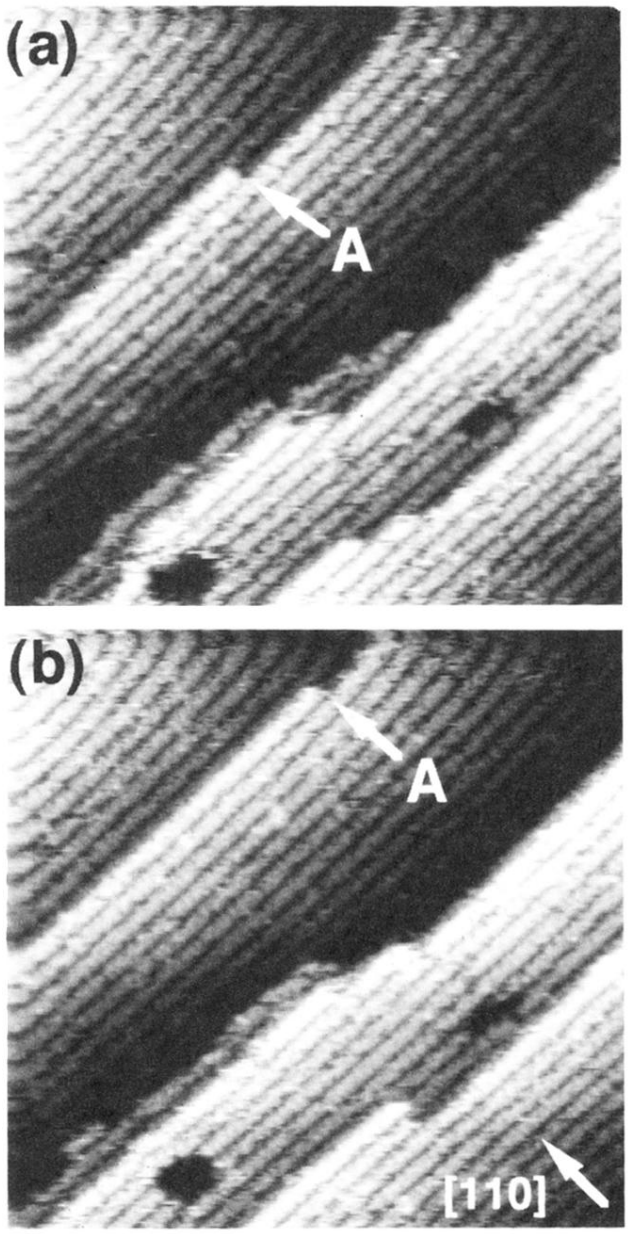

FIG. 17. The STM images of an InAs (001) surface obtained at 330 °C at 35-s intervals. The image area is 50×50 nm, the bias voltage was −3.5 V, and the tip current was 0.08 nA.

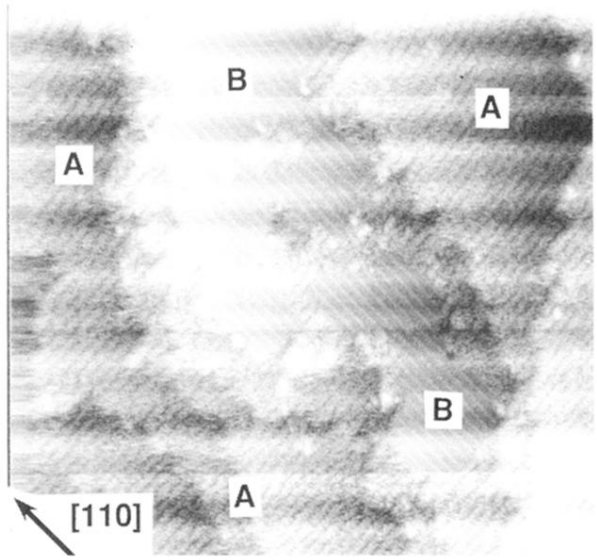

FIG. 18. The STM image of an InAs (001) surface obtained at 350 °C. The image area is 100×100 nm, the bias voltage was −2.0 V, and the tip current was 0.08 nA.

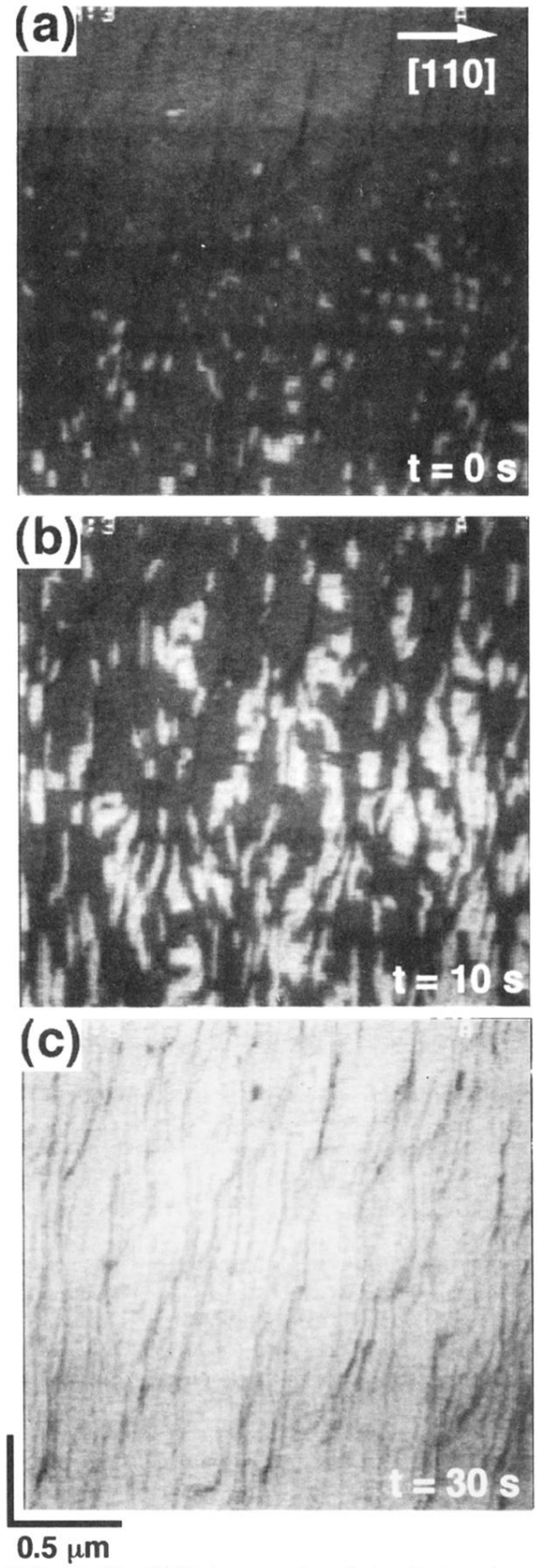

FIG. 19. The SEM images of an InAs 1°-*A* surface during the transition from (2×4) to (4×2) structures. (b) was obtained 10 s after (a), and (c) was obtained 20 s after (b). Steps proceed downward from left to right.

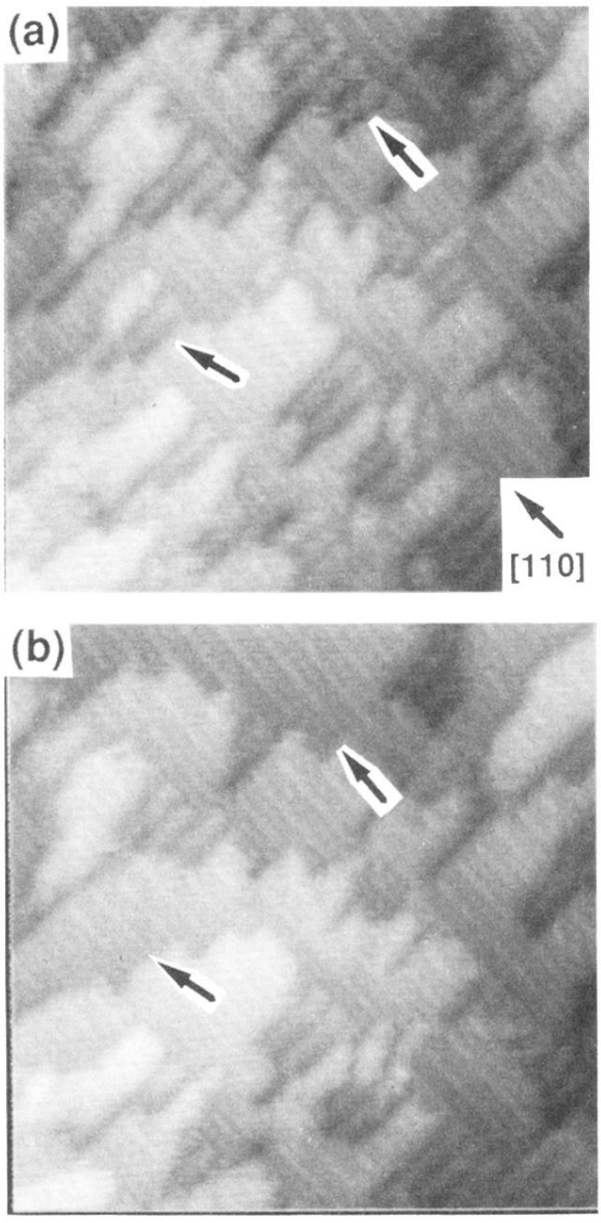

FIG. 23. The STM images of an InAs (001) surface obtained at 350 °C at an interval of 35 s. The image area is 40×40 nm, the bias voltage was −2.5 V, and the tip current was 0.1 nA.

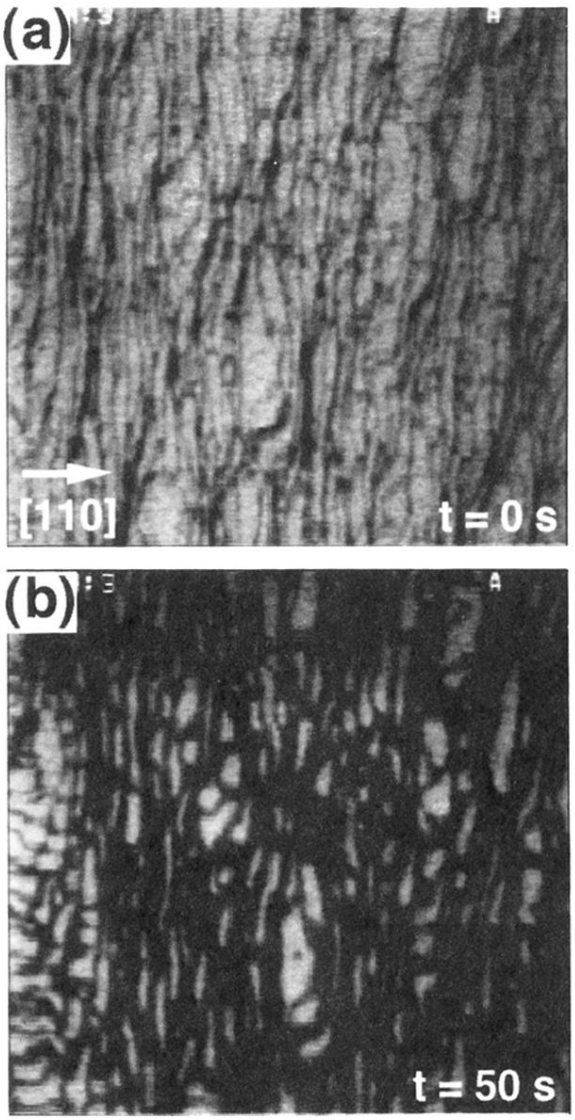

FIG. 24. Secondary electron image of an InAs (001) surface during the transition from a (4×2) to a (2×4) surface. (a) was obtained just after the transition began, and (b) was obtained 50 s later. The image size is 2.3 μm (horizontal) × 2.9 μm (vertical).

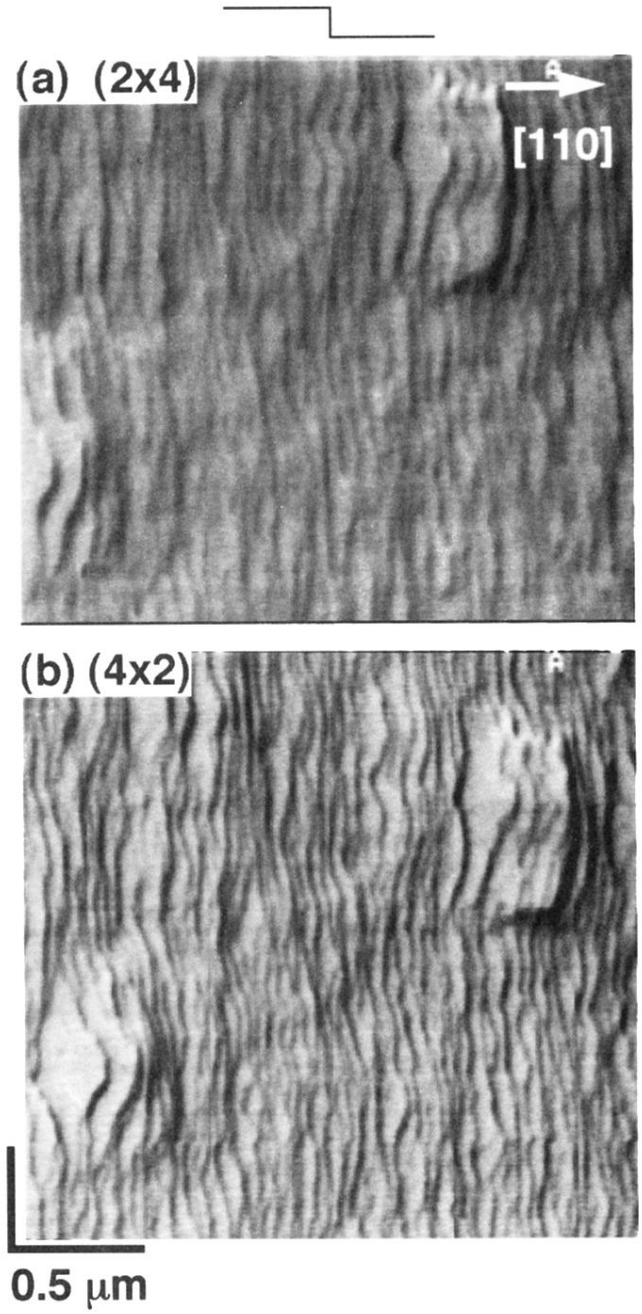

FIG. 25. The SEM images of an InAs 2°-*A* surface with (a) (2×4) and (b) (4×2) structures. Steps proceed downward from left to right.

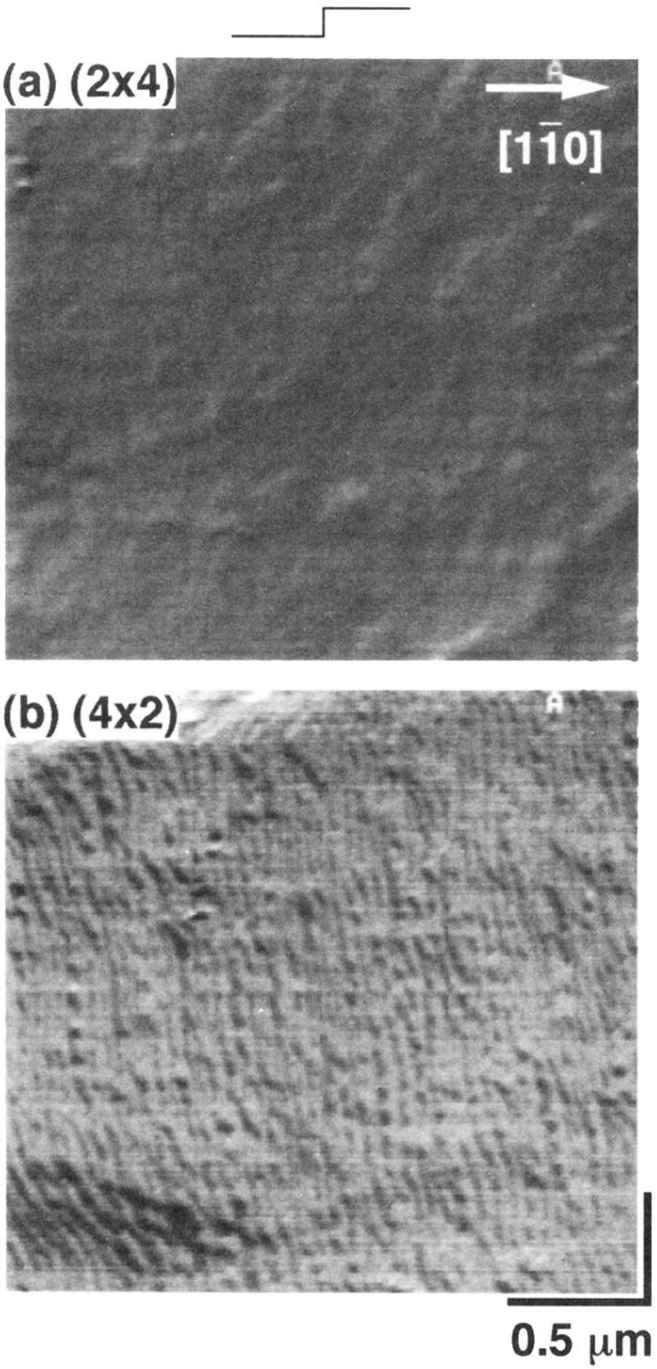

FIG. 26. The SEM images of an InAs 2°-B surface with (a) (2×4) and (b) (4×2) structures. Steps proceed downward from right to left.

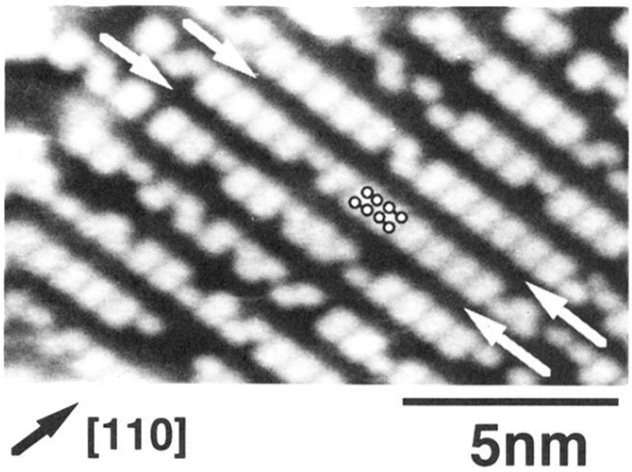

FIG. 9. Scanning tunneling microscopy image of an InAs (2×4) surface just after growth. The sample bias was −3.0 V and the tunneling current was 0.08 nA.